

PLATINUM-GROUP-ELEMENT MINERALIZATION IN LODE AND PLACER DEPOSITS ASSOCIATED WITH THE TULAMEEN ALASKAN-TYPE COMPLEX, BRITISH COLUMBIA

GRAHAM T. NIXON

Ministry of Energy, Mines and Petroleum Resources, Geological Survey Branch, Parliament Buildings,
Victoria, British Columbia V8V 1X4

LOUIS J. CABRI AND J.H. GILLES LAFLAMME

Canada Centre for Mineral and Energy Technology, 555 Booth Street, Ottawa, Ontario K1A 0G1

ABSTRACT

Textures and compositions of platinum-group minerals (*PGM*) and coexisting silicate, oxide and base-metal minerals have been examined in platinum-group-element-enriched chromitites of the Alaskan-type Tulameen complex and spatially associated placers. Major objectives of this study were to compare the *PGM* in bedrock and placer occurrences and to evaluate their origin. The common Pt-Fe-Ni-Cu alloys in chromitites are tentatively identified as "tetraferroplatinum" [Pt(Fe,Ni,Cu)] and "isoferroplatinum" [Pt_{2.5}(Fe,Ni,Cu)_{1.5}], whereas placers commonly contain isoferroplatinum [Pt₃Fe to Pt_{2.6}(Fe,Cu,Ni)_{1.4}], native and ferroan platinum. Most alloys (with the notable exception of tulameenite and platinian copper), laurite and erlichmanite are considered to represent a primary high-temperature paragenesis. Other *PGM*, most notably Pt arsenides and antimonides, Rh-Ir sulfarsenides and platinian copper, are secondary, and formed by metasomatic replacement and localized remobilization of *PGE* during serpentinization and regional metamorphism. A low-temperature hydrothermal origin also is indicated for small quantities of base-metal sulfides (pyrite, millerite-heazlewoodite, pentlandite, violarite, bravoite, chalcopyrite, and an undetermined Ni-Co-Fe sulfide), antimonides (breithauptite, Ni₂Sb and Ni₃Sb), arsenides [maucherite(?) and Ni₇As₃], native copper, native silver, magnetite, and copper and nickel oxides. Cumulus chromite embedded in platinum alloy in placer nuggets has high Cr (35–50 wt. % Cr₂O₃), Fe³⁺ (12–28 wt. % Fe₂O₃) and Cr/(Cr + Al) ratios (0.79–0.83), and low Al (6–9 wt. % Al₂O₃), and falls within the compositional field defined by Tulameen chromitites. Olivine in these nuggets is anomalously forsteritic (Fo_{93–95}) compared to compositions in Tulameen dunite (Fo_{88–91}), but similar to olivine compositions (Fo_{92–95}) found in chromitites. These data indicate quite conclusively that the *PGE* mineralization in the placers was derived from chromitites in the dunite core of the Tulameen complex. Other silicate inclusions in the nuggets comprise primary clinopyroxene (Mg- to Fe-rich diopside), magnesian phlogopite to Fe-rich biotite, ferroan pargasitic hornblende and plagioclase, and secondary sericitic mica, chromian chlorite and Cr-bearing epidote. The primary mineral assemblage evidently crystallized from inclusions of silicate melt trapped within platinum alloy at the time of chromitite formation; the secondary minerals formed during subsequent greenschist-facies metamorphism. The origin of *PGE*-enriched chromitites in the Tulameen and other Alaskan-type intrusions is related

to segregation of predominantly Pt-Fe alloys directly from the melt during conditions that enhanced the precipitation of chromite [e.g., increase in $f(\text{O}_2)$]. There is no evidence for high-temperature subsolidus concentration of *PGE* by either exsolution from chromite or desulfurization of primary magmatic sulfides.

Keywords: platinum-group elements, platinum-group minerals, electron microprobe, platinum nuggets, placers, provenance, platinum mineralization, sulfides, mineralogy, Tulameen, Alaskan-type complex, British Columbia.

SOMMAIRE

Nous avons étudié les textures et la composition des minéraux du groupe du platine (*MGP*) et les silicates, oxydes, et minéraux des métaux de base coexistants dans les chromitites enrichies en éléments du groupe du platine (*EGP*) du complexe de Tulameen (Colombie-Britannique), de type Alaska, et les graviers platinifères qui lui sont associés. Notre but principal était de comparer les *MGP* dans les roches et dans les graviers, afin d'en évaluer l'origine. Les alliages de Pt-Fe-Ni-Cu trouvés dans les chromitites sont "tétraferroplatine" [Pt(Fe, Ni, Cu)] et "isoferroplatine" [Pt_{2.5}(Fe,Ni,Cu)_{1.5}], tandis que les graviers contiennent isoferroplatine [Pt₃Fe à Pt_{2.6}(Fe,Cu,Ni)_{1.4}], platine natif et platine ferrifère. La plupart des alliages (exceptions faites de la tulameenite et du cuivre platinifère), ainsi que laurite et erlichmanite, représenteraient une paragenèse primaire, de haute température. Tous les autres *MGP*, notamment les arsénures et les antimoniures de Pt, les sulfarséniures de Rh-Ir et le cuivre platinifère, seraient secondaires, résultant d'un remplacement métasomatique et d'une remobilisation locale des *EGP* au cours de la serpentinisation et d'un épisode de métamorphisme régional. Une origine hydrothermale est indiquée pour les petites quantités de sulfures des métaux de base (pyrite, millerite-heazlewoodite, pentlandite, violarite, bravoite, chalcopyrite, ainsi qu'un sulfure de Ni-Co-Fe non caractérisé), d'antimoniures (breithauptite, Ni₂Sb et Ni₃Sb), d'arsénures [maucherite(?) et Ni₇As₃], cuivre et argent natifs, magnétite, et les oxydes de Cu et Ni. La chromite cumulative qui se trouve dans les pépites de l'alliage de platine est riche en Cr (35–50% de Cr₂O₃, en poids) et Fe³⁺ (12–28% de Fe₂O₃), et possède un rapport Cr/(Cr + Al) élevé (0.79–0.83) et une faible teneur en Al (6–9% de Al₂O₃). Sa composition correspond au champ de la chromite des chromitites de Tulameen.

L'olivine des pépites est fortement magnésienne (FO_{93-95}) comparée aux compositions typiques de la dunite (FO_{88-91}), mais elle ressemble à celle des chromitites (FO_{92-95}). Ces données démontrent nettement que la minéralisation en EGP des alluvions a été dérivée des chromitites du coeur dunitique du complexe de Tulameen. Les autres inclusions de silicates jugés primaires dans les pépites consistent de clinopyroxène (diopside riche en Mg ou Fe), phlogopite magnésienne à biotite ferrifère, hornblende pargasitique ferrifère, et plagioclase. Les minéraux secondaires sont mica séricitique, chlorite et épidote chromifères. Les minéraux primaires ont cristallisé à partir d'inclusions de magma occluses dans l'alliage de platine lors de la formation des chromitites. Les minéraux secondaires sont apparus lors d'un épisode postérieur de métamorphisme (facies schistes verts). L'origine des chromitites enrichies en EGP à Tulameen et dans les autres massifs du type Alaska est liée à la ségrégation des alliages de Pt-Fe, surtout, directement à partir du magma pendant que les conditions étaient propices à la précipitation massive de chromite [e.g., augmentation en $f(O_2)$]. Il n'y a aucun signe d'une concentration des EGP à température élevée par exsolution dans la chromite ou par désulfuration des sulfures magmatiques primaires.

(Traduit par la Rédaction)

Mots-clés: éléments du groupe du platine, minéraux du groupe du platine, microsonde électronique, pépites de platine, graviers platinifères, provenance, minéralisation en platine, sulfures, minéralogie, Tulameen, massif du type Alaska, Colombie-Britannique.

INTRODUCTION

In situ platinum-group-element (PGE) mineralization and derived placers are well known in Alaskan-type intrusive complexes and their environs of stable platform or mobile belts (e.g., Aldan shield and Ural Mountains, USSR; Youbdo, Ethiopia; Choco District, Columbia and Goodnews Bay, Alaska; cf. Cabri 1981). In southern British Columbia, platinum- and gold-bearing placers in the Tulameen-Similkameen river systems historically have been significant producers of PGE, yielding an estimated 620 kg of impure platinum between 1889 and 1936 (O'Neill & Gunning 1934, Rice 1947). The source of the platinum has been traced to ultramafic rocks of the Tulameen complex, a mafic-ultramafic intrusion of the Alaskan type, whereas the origin of the gold has traditionally been related to a younger episode of regional vein-type mineralization. According to Rice (1947), the ratio of alluvial platinum to gold increases from about 1:4 in the lower reaches of the Tulameen and Similkameen rivers to about 1:1 in the vicinity of the ultramafic complex. Renewed interest in platinum metals in recent years has promoted exploration for primary platinum mineralization in the Tulameen and other Alaskan-type complexes.

Modern studies of the Tulameen district have

documented a number of discrete platinum-group minerals (PGM) in both placer and lode occurrences (e.g., Cabri *et al.* 1973, Raicevic & Cabri 1976, St. Louis *et al.* 1986). In particular, St. Louis *et al.* (1986) showed that chromitites in the dunitic core of the Tulameen complex are anomalously enriched in platinum-group elements (PGE) relative to their silicate host-rocks, and identified several species of PGM, including Pt-Fe alloys and platinum antimonides and arsenides. In the study described below, we have used scanning electron microscopy and quantitative electron-microprobe methods to further characterize the speciation and composition of the PGM and coexisting spinels, silicates and various base-metal minerals in Tulameen chromitites and associated placer material. These data are used to examine the origin of the PGE mineralization in both lode and placer deposits, and to construct a paragenetic scheme for the PGM. In addition, the data demonstrate quite convincingly that *in situ* PGE mineralization and alluvial platinum share a common heritage. The latter conclusion has important implications for future exploration for PGE in the Tulameen region.

GEOLOGICAL SETTING OF THE TULAMEEN COMPLEX

The geology of the Tulameen mafic-ultramafic complex (Fig. 1) has been described by Camsell (1913), Rice (1947), Findlay (1963, 1969), Nixon & Rublee (1988) and Nixon (1988), although Findlay's accounts remain the most comprehensive to date. The complex forms an elongate body some 20 km in length that is concordant with the northwesterly trending regional structures. Host rocks of the Nicola Group comprise greenschist-grade, metavolcanic and metasedimentary rocks that lie in fault contact with the Tulameen complex (Fig. 1). A crude outward zonation of common Alaskan-type lithologies is exposed, ranging from a dunite "core" at the northern end of the complex, through an envelope of olivine clinopyroxenite and clinopyroxenite, to hornblende clinopyroxenite, hornblendite and hornblende-feldspar pegmatite near the margins; wehrlite is notably rare. The main mass of gabbroic to syenitic rocks is eccentrically distributed at the southern and eastern margins of the complex. Contacts between the feldspathic and ultramafic rocks display ambiguous intrusive relationships. Primary mesoscopic layering, such as that so spectacularly developed at the classic locality of Duke Island in southeastern Alaska (Irvine 1974), is poorly developed. Early cumulate minerals are represented by forsteritic olivine, chromite, diopsidic clinopyroxene and rare phlogopitic mica, whereas hornblende, biotite, magnetite and plagioclase generally predominate in the more evolved rock-types. In common with other Alaskan-type complexes, orthopyroxene is

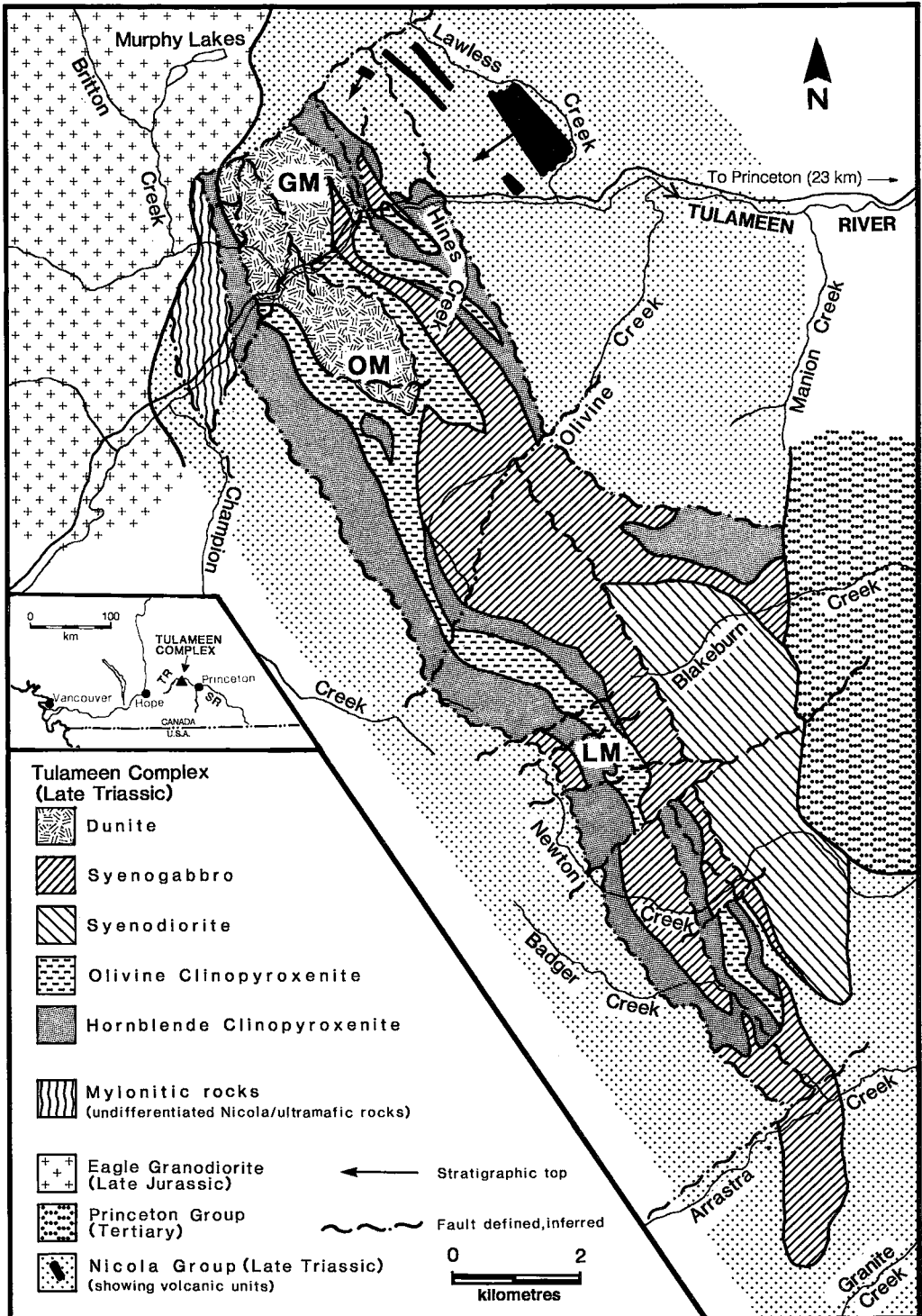


FIG. 1. Location and generalized geology of the Tulameen ultramafic complex, modified after Findlay (1963) and Nixon (1988). GM, Grasshopper Mountain; OM, Olivine Mountain; LM, Lodestone Mountain; TR, Tulameen River; and SR, Similkameen River (inset).

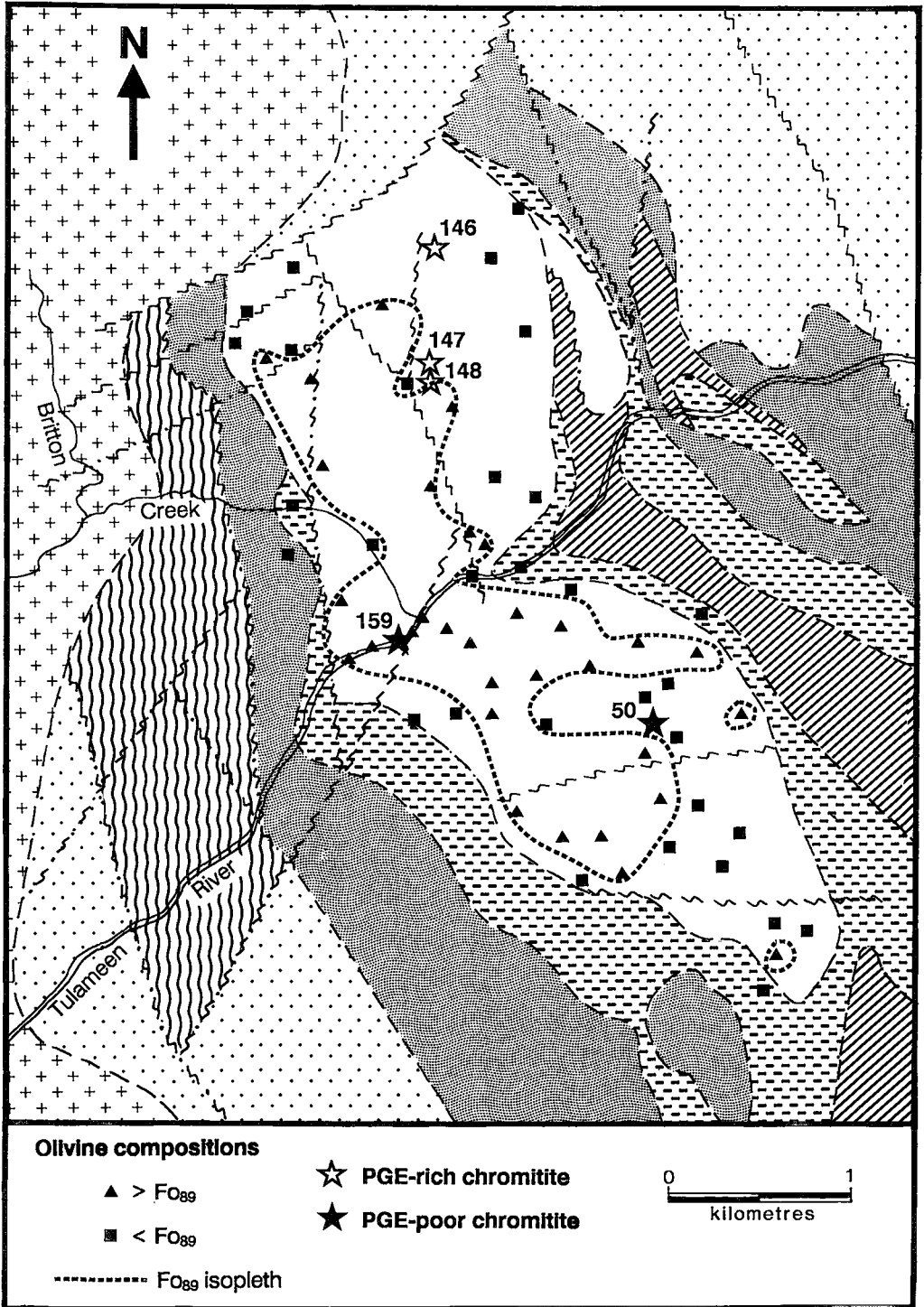


FIG. 2. Geological map of the dunite core of the Tulameen complex, showing olivine compositions (after Findlay 1963) and chromitite localities documented in this study. Total range of olivine compositions in dunite is FO_{88} – FO_{92} . Symbols as in Figure 1 except for dunite core.

characteristically absent from ultramafic cumulates, a feature that has been taken to indicate an alkaline affinity (Findlay 1963). Recently, Mortimer (1986) suggested that the intrusion was coeval with Late Triassic (Carnian–Norian) calc-alkaline to shoshonitic arc-related rocks of the Nicola Group. Recent U–Pb isotopic work on zircon from syenogabbros at the eastern margin of the complex yields a slightly discordant date of 204–212 Ma (Late Triassic – Early Jurassic; Rublee & Parrish 1990).

SAMPLE DESCRIPTION

Placer nuggets

The nuggets examined in this study were obtained from a variety of sources; some have been studied previously by Cabri and co-workers (Cabri *et al.* 1973, Harris & Cabri 1973, Cabri & Hey 1974, Cabri & Feather 1975, Raicevic & Cabri 1976). The samples comprise rounded to subrounded monomineralic grains or polyminerallitic aggregates that reach 7 mm in diameter and have a metallic luster. The “Lincoln” nugget was purchased from a local collector and is named for the “Lincoln mine”, a former placer operation on the Tulameen River situated about 0.8 km below the mouth of Britton Creek (formerly Eagle Creek). The “Holland” nugget was obtained from the Tulameen River by the late Dr. S. S. Holland, formerly of the B. C. Department of Mines (Ministry of Energy, Mines and Petroleum Resources). Sample M12410 is a vial of numerous placer grains obtained from the Royal Ontario Museum, Toronto. This material is considered to have come from a site located on the Tulameen River just upstream of the junction with Lawless (Bear) Creek (Fig. 1). Three relatively large nuggets (M12410–1, –2, and –3) were selected for study.

Tulameen chromitites

Chromitite specimens were collected from three different sites on Grasshopper Mountain in the northern part of the dunite body (Fig. 2). Previous work by Mr. D. Bohme, formerly of Newmont Exploration Limited, had outlined areas of platinumiferous chromitite on the southern slopes of Grasshopper Mountain, and earlier St. Louis *et al.* (1986) had documented PGE-rich chromitites in a northeast–southwest traverse across the summit of the mountain. In this study, chromitites from Grasshopper Mountain were resampled as part of a recent effort to more thoroughly evaluate the PGE potential of Alaskan-type complexes in British Columbia (Nixon 1990).

The chromitites typically form bulbous or irregular masses less than 10 cm across, or occur as thin, discontinuous schlieren 1–4 cm in width by up to 4

m in length. The core of these bodies consists of massive chromite that has indistinct crystal outlines and is locally cross-cut by irregular fractures. The margins of chromitites contain large (1–2 mm) subhedral to euhedral chromite crystals interspersed with olivine, and exhibit a sharp gradation into tiny (<20 μm) grains of euhedral spinel (1 vol. %) in enveloping dunite. The margins of some schlieren exhibit rings of euhedral chromite granules that surround larger crystals of cumulate olivine, similar to textures documented elsewhere (*e.g.*, the Turnagain Alaskan-type complex in north-central British Columbia; Clark 1975, 1980). The formation of massive chromitite appears to have proceeded *via* coalescence of chromite grains of variable size during recrystallization and annealing at elevated temperatures, in the manner described by Eales (1987). Disruption and redistribution of chromitite horizons within the dunite appear to have been accomplished by intermittent slumping and redeposition of formerly stratified cumulates at a relatively early stage of solidification of the magma chamber (Nixon & Rublee 1988).

Chromitite geochemistry

Abundances of noble metals in the three chromi-

TABLE 1. ABUNDANCES* OF PLATINUM-GROUP ELEMENTS IN CHROMITITES OF THE TULAMEEN COMPLEX

Sample	Pt	Pd	Rh	Ru	Ir	Os
GN87-146 ¹	2500	5	20	<10	17	8
GN87-146 ²	9297	73	-	-	-	-
GN87-146 ³	3189	23	-	-	-	-
GN87-147 ¹	5600	75	56	<5	140	20
GN87-147 ²	7953	59	-	-	-	-
GN87-147 ³	5527	47	-	-	-	-
GN87-147 ³	5380	39	(duplicate subsample)			
GN87-147 ⁴	8348	<30	70	<15	243	50
GN87-148 ¹	5300	12	67	50	220	25
GN87-148 ²	4762	19	-	-	-	-
GN87-148 ³	7398	<15	68	<20	247	48
Average chromitite**	3410(2220)	<83	40(20)	-	100(40)	40(20)

* Concentrations in ppb. - not determined.

Analyses made on 50-g splits of rock powder using fire-assay preconcentration of noble metals followed by:

- 1 instrumental neutron activation (Activation Laboratories Ltd., Ancaster, Ontario)
- 2 atomic absorption spectrometry - graphite furnace finish (Analytical Laboratories, B. C. Ministry of Energy, Mines and Petroleum Resources, Victoria, British Columbia)
- 3 inductively coupled plasma mass spectrometry (Geochemical Laboratories, Geological Survey of Canada, Ottawa)
- 4 instrumental neutron activation (Institut national de la recherche scientifique, Georesources, Sainte-Foy, Quebec)

** Mean value (standard error of the mean) from St. Louis *et al.* 1986, Table 4.

Sample locations: GN87-146: 230 m NW of Grasshopper Mountain summit at 1420 m (Lat. 49°32.7'N, Long. 120°53.9'W); GN87-147: southern slope of Grasshopper Mountain at 1370 m (Lat. 49°32.3'N, Long. 120°54'W); GN87-148: 740 m SSW of Grasshopper Mountain summit at 1340 m (Lat. 49°32.2'N, Long. 120°54'W).

tite samples selected for study are presented in Table 1. The *PGE* were preconcentrated by fire assay using generous (50 g) splits of rock powder and subsequently analyzed by three different analytical techniques (*cf.* footnotes to Table 1). The results show that the chromitites are highly enriched in Pt (2500–9300 ppb) and, to a much lesser extent, Ir (<250 ppb), relative to the other *PGE*, especially ruthenium, which is generally below detection limits. (Pt + Pd)/(Ru + Os + Ir) and Pt/Pd ratios are extremely high. The new analytical results compare well with previously published data on the Grasshopper Mountain chromitites (St. Louis *et al.* 1986) (Table 1). Background Pt values in dunite and peridotite are approximately 70–80 ppb (Findlay 1963). The anomalous enrichment of Pt in the chromitites is related to the occurrence of a number of distinct species of *PGM*, the most abundant of which are Pt–Fe–Ni–Cu alloys. These geochemical and mineralogical characteristics are typical of Alaskan-type intrusions in general (Cabri 1981). The considerable range of *PGE* abundances evident in any one sample primarily reflects the practical difficulties of sampling a medium in which the *PGE* occur as discrete and dispersed *PGM*.

SAMPLE PREPARATION AND MICROPROBE TECHNIQUES

Chromitite specimens were initially examined in polished thin sections with a Nanolab 7 scanning electron microscope at the University of British Columbia. Subsequently, the nuggets and six chromitite chips from three samples (GN87–146, –147, and –148) were selected for quantitative analysis, and sliced and mounted in cold-setting araldite. The samples were polished on a temperature-controlled Dürer polisher using lead laps, with final buffing using 0.05 μm gamma alumina (Laflamme 1990).

Electron-microprobe analyses were done at CANMET on a JEOL 733 microanalyzer system. The silicate and spinel analyses were carried out by energy-dispersion spectrometry at 15 kV, with a beam (Faraday cup) current of 12 nA, and using the following X-ray lines (and standards): FeK α (metal or amphibole #1), CrK α , NiK α and ZnK α (metals), AlK α (Al₂O₃), SiK α (SiO₂), MnK α (rhodochrosite), TiK α (TiO₂), MgK α (MgO), KK α (orthoclase), CaK α (wollastonite) and NaK α (NaNbO₃). Concentrations of Ni and Zn were determined by wavelength-dispersion spectrometry. Counting times were of the order of 100 s. Analyses of all the *PGM* and *PGE*-bearing minerals were carried out by wavelength-dispersion spectrometry at 20 kV, with a beam current of 20 nA, using the following X-ray lines (and standards): PtL α and FeK α (PtFe or Pt₃Fe), PdL α , RhL α , RuL α , IrL α , OsM α , CuK α , NiK α and SbL α (metals), AsL α (InAs), and SK α (pyrite). Raw data

were corrected using the ZAF program supplied by Tracor Northern, and additional corrections were performed for enhancement of the following primary X-ray lines by secondary lines: RuL β ₁ and PtM₂N₄ on RhL α ₁, IrLL on CuK α , RuL β ₂ and RhL β ₁ on PdL α ₁, and RuL α ₁₁ and SbL β ₁ on AsL α . Additional electron-microprobe analyses were performed at Queen's University on spinel and olivine in chromitites, dunites and clinopyroxenites using an ARL-SEM-Q microanalyzer fitted with an energy-dispersion spectrometer and a Tracor Northern X-ray analysis system. Ten-element analyses were performed simultaneously using an accelerating potential of 15 kV, a beam current of about 20 nA, and counting times of 200 s. Materials used as standards include synthetic glass (Queen's University reference number S-204), chromite (S-164) and olivine (S-68). X-ray intensities were corrected for matrix effects using the procedures of Bence & Albee (1968) and alpha correction factors of Albee & Ray (1970).

PETROGRAPHY AND MINERALOGY OF TULAMEEN CHROMITITES

Chromitites within the dunite core of the Tulameen complex contain essential chromiferous spinel and minor, variably serpentinized olivine. *PGE*-rich chromitites exhibit a variety of discrete *PGM*, the proportion of which, in replicate polished sections, is highly variable and no doubt responsible for the significant range of *PGE* abundances noted above. Both *PGE*-rich and *PGE*-poor chromitites contain minor quantities of base-metal sulfides and arsenides, and trace amounts of native metals and metal oxides. Serpentinization is generally quite pronounced in the dunite within a few millimeters of the chromitite contact. Chromitite pods also are commonly traversed by hairline fractures filled with serpentine, chlorite, magnetite, carbonate and minor base metals and base-metal sulfides.

Platinum-group minerals

The *PGE* in chromitites are distributed primarily among Pt–Fe–Ni–Cu alloys, the most common *PGM*, geversite, Rh–Ir sulfarsenides, sperrylite, platinum copper, platinum oxide, erlichmanite and laurite, listed in order of decreasing abundance. The *PGM* are found as discrete grains or complex polymineralic intergrowths.

The nomenclature of the Pt–Fe–Ni–Cu alloys is problematical since there is a lack of data for phase relations in this system, and even relations along the Pt–Fe binary join are inadequately known (Cabri & Feather 1975). Identification of platinum alloy species requires characterization of crystal structure as well as phase composition (Cabri & Feather 1975), but no X-ray-diffraction data have been obtained

TABLE 2A. ELECTRON-MICROPROBE DATA ON PLATINUM ALLOY INCLUSIONS IN CHROMITITES, TULAMEEN COMPLEX

Anal. No.	Grain Size (μm)	Weight per cent									Atomic proportions												
		Pt	Rh	Pd	Ir	Os	Fe	Cu	Ni	Sb	Totals	Pt	Rh	Pd	Ir	Os	Sum	Fe	Cu	Ni	Sb	Sum	
1. Pt(Fe,Ni,Cu) - tetraferroplatinum?																							
1	12 x 32	76.8	n.d.	n.d.	0.46	n.d.	13.4	4.7	4.1	0.23	99.69	1.007			0.006	1.013	0.614	0.189	0.179	0.005	0.987		
2*	4 x 8	76.6	0.26	0.30	0.25	n.d.	13.7	3.2	4.6	n.d.	98.91	1.016	0.006	0.007	0.003	1.032	0.634	0.130	0.203		0.967		
3	4 x 8	77.2	0.34	0.30	0.38	n.d.	13.9	2.9	4.3	n.d.	99.32	1.026	0.009	0.007	0.005	1.047	0.645	0.118	0.190		0.953		
4*	6 x 8	77.1	0.26	0.29	0.17	n.d.	13.0	3.2	4.7	n.d.	98.72	1.034	0.007	0.007	0.002	1.050	0.609	0.132	0.210		0.951		
5	15 x 20	72.6	0.43	0.50	3.50	n.d.	14.8	3.3	3.9	n.d.	99.03	0.951	0.011	0.012	0.046	1.020	0.677	0.133	0.170		0.980		
6	10 x 10	73.3	0.38	0.50	1.90	n.d.	14.2	2.8	5.9	n.d.	98.98	0.948	0.009	0.012	0.025	0.994	0.641	0.111	0.254		1.006		
7	20 x 25	74.2	0.40	0.53	2.80	n.d.	15.2	3.2	3.4	n.d.	99.73	0.970	0.010	0.013	0.037	1.030	0.694	0.128	0.148		0.970		
8	8 x 15	71.5	0.57	0.49	4.80	n.d.	14.7	2.8	5.0	n.d.	99.86	0.923	0.014	0.012	0.063	1.012	0.663	0.111	0.215		0.989		
9	5 x 6	74.5	0.31	0.15	0.35	n.d.	13.7	3.2	5.3	0.08	97.59	0.986	0.008	0.004	0.005	1.003	0.633	0.130	0.233	0.002	0.998		
10	3 x 5	74.6	0.46	0.35	0.59	n.d.	13.9	2.8	5.1	n.d.	97.80	0.989	0.012	0.008	0.008	1.017	0.644	0.114	0.225		0.983		
11	5 x 6	75.0	0.36	0.33	1.40	n.d.	13.9	2.3	4.4	n.d.	97.69	1.014	0.009	0.008	0.019	1.050	0.656	0.095	0.198		0.949		
2. Pt_{2.5}(Fe,Ni,Cu)_{1.5} - isoferroplatinum?																							
12	10 x 10	82.9	0.63	0.43	0.60	0.21	10.9	1.1	2.6	n.d.	99.37	2.440	0.035	0.023	0.018	0.006	2.522	1.121	0.099	0.255		1.475	
13*	4 x 8	81.2	0.75	0.50	0.56	n.d.	11.5	1.0	3.2	n.d.	98.71	2.350	0.041	0.027	0.017		2.435	1.165	0.089	0.308		1.562	
14	8 x 9	83.4	0.67	0.45	0.51	n.d.	11.0	1.2	2.7	n.d.	99.93	2.430	0.037	0.024	0.015		2.506	1.121	0.107	0.262		1.490	
15*	10 x 10	81.8	0.60	0.48	0.50	n.d.	11.2	2.1	2.9	n.d.	99.58	2.345	0.033	0.025	0.015		2.418	1.121	0.185	0.276		1.582	
16*	6 x 8	80.8	0.56	0.50	0.24	n.d.	12.5	1.1	2.6	n.d.	98.30	2.330	0.031	0.026	0.007		2.394	1.259	0.097	0.249		1.605	
17	5 x 5	81.0	0.52	0.20	3.60	n.d.	11.4	0.5	1.2	n.d.	98.39	2.470	0.030	0.011	0.111		2.622	1.214	0.044	0.122		1.380	
3. Pt₂(Fe,Cu,Ni,Sb)₂ - tulameenite?																							
18	30 x 35	71.4	n.d.	0.65	n.d.	n.d.	5.5	12.9	2.0	6.90	99.25	1.915		0.032		1.947	0.515	1.062	0.178	0.297		2.052	
19	10 x 10	73.8	0.44	0.39	0.29	0.33	11.1	9.7	2.9	n.d.	98.95	1.915	0.022	0.019	0.008	0.009	1.973	1.006	0.773	0.250		2.029	

n.d. = not detected. Ru was not detected; minimum detection limits in wt. % are: Rh, Pd, Ru 0.05; Os 0.10; and Sb 0.07. * and + = coexisting alloys.

1 - With minor hollingworthite in silicate in contact with chromite; 2 - With isoferroplatinum and erlichmanite; 4 - With isoferroplatinum, Co-Ni-Fe sulphide and laurite; 5 - With platinum copper; 13 - c.f. 2; 14 - With some laurite; 15 - With tulameenite and platinum copper; 16 - c.f. 4; 18 - With some platinum copper; 19 - c.f. 15. Sample key: Analyses 1-4, 12-16, 18, 19: GN87-146B; Analyses 5-8: GN87-147B; Analyses 9-11: GN87-146A; Analysis 17: GN87-148A.

TABLE 2B. ELECTRON-MICROPROBE DATA ON PLATINUM ALLOYS IN PLACER NUGGETS

Anal. No.	Weight per cent									Atomic proportions										
	Pt	Rh	Pd	Ir	Fe	Cu	Ni	Sb	Totals	Pt	Rh	Pd	Ir	Sum	Fe	Cu	Ni	Sb	Sum	
1. Pt(Fe,Cu,Ni) - tetraferroplatinum?																				
1	71.0	0.62	n.d.	6.5	16.4	4.6	0.22	n.d.	99.34*	0.94	0.01		0.09	1.04	0.76	0.19	0.01		0.96	
2. Pt₃Fe and Pt_{2.6}(Fe,Cu,Ni)_{1.4} - isoferroplatinum?																				
2	79.0	0.62	0.17	7.0	12.3	0.95	0.20	n.d.	100.24*	2.36	0.03	0.01	0.21	2.61	1.28	0.09	0.02		1.39	
3	79.2	0.66	0.18	7.0	12.8	0.92	0.21	n.d.	100.97*	2.33	0.04	0.01	0.21	2.59	1.31	0.08	0.02		1.41	
4	90.2	-	-	n.d.	9.1	0.07	0.22	0.14	99.73	2.93				2.93	1.03	0.01	0.02	0.01	1.07	
5	88.0	-	-	2.3	9.0	0.11	0.13	0.11	99.65	2.87			0.08	2.95	1.02	0.01	0.01	0.01	1.05	
6	88.6	-	-	2.2	8.7	0.15	0.09	0.24	99.98	2.91			0.07	2.98	0.99	0.01	0.01	0.01	1.02	
3. Pt₂FeCu - tulameenite?																				
7	69.9	0.60	n.d.	6.5	11.7	11.0	0.20	n.d.	99.90*	1.83	0.03		0.17	2.03	1.07	0.88	0.02		1.97	

Analyses 1, 2, 3, 7 from M12410 nugget #3; analyses 4, 5, 6 from Holland nugget. n.d. = not detected; - = not determined; * = Os not detected.

owing to the small grain-size of the PGM. However, based on considerations of stoichiometry and previous work, we tentatively recognize three species of alloys (Table 2A).

Pt-Fe-Ni-Cu alloys, or simply platinum alloys, have been positively identified in more than 30 euhedral to subhedral grains (<35 μm), and most are encapsulated by chromite (Figs. 3, 4, 5). Their compositions are plotted in Figure 6. Most grains plot near the center of a triangle bounded by PtFe (tetraferroplatinum), Pt₂FeCu (tulameenite) and Pt₂NiFe (ferronickelplatinum) (Fig. 6D) and are not unlike alloy compositions from other occurrences world-wide such as Noril'sk, USSR (Genkin & Evstigneeva 1986) and the former Onverwacht mine,

Transvaal (Cabri *et al.* 1977). The latter authors reported on the composition of a tetragonal alloy approximately midway along the join Pt₂FeCu-Pt₂NiFe (Pt₂FeNi_{0.5}Cu_{0.5}) (Fig. 6D) and suggested that it might represent a Ni- and Cu-rich variety of tetraferroplatinum.

The majority of the grains of Pt-Fe-Ni-Cu alloys analyzed in chromitites are stoichiometrically close to Pt(Fe,Ni,Cu), with minor Ir (0.17-4.8 wt.%), Pd (<0.53 wt.%) and Rh (<0.57 wt.%) substituting for Pt (Table 2A). We tentatively regard this composition as representative of *tetraferroplatinum*, even though significant quantities of Ni (3.4-5.9 wt.%) and Cu (2.3-4.7 wt.%) distinguish it from the ideal PtFe stoichiometry. Abundances of Os and Ru are

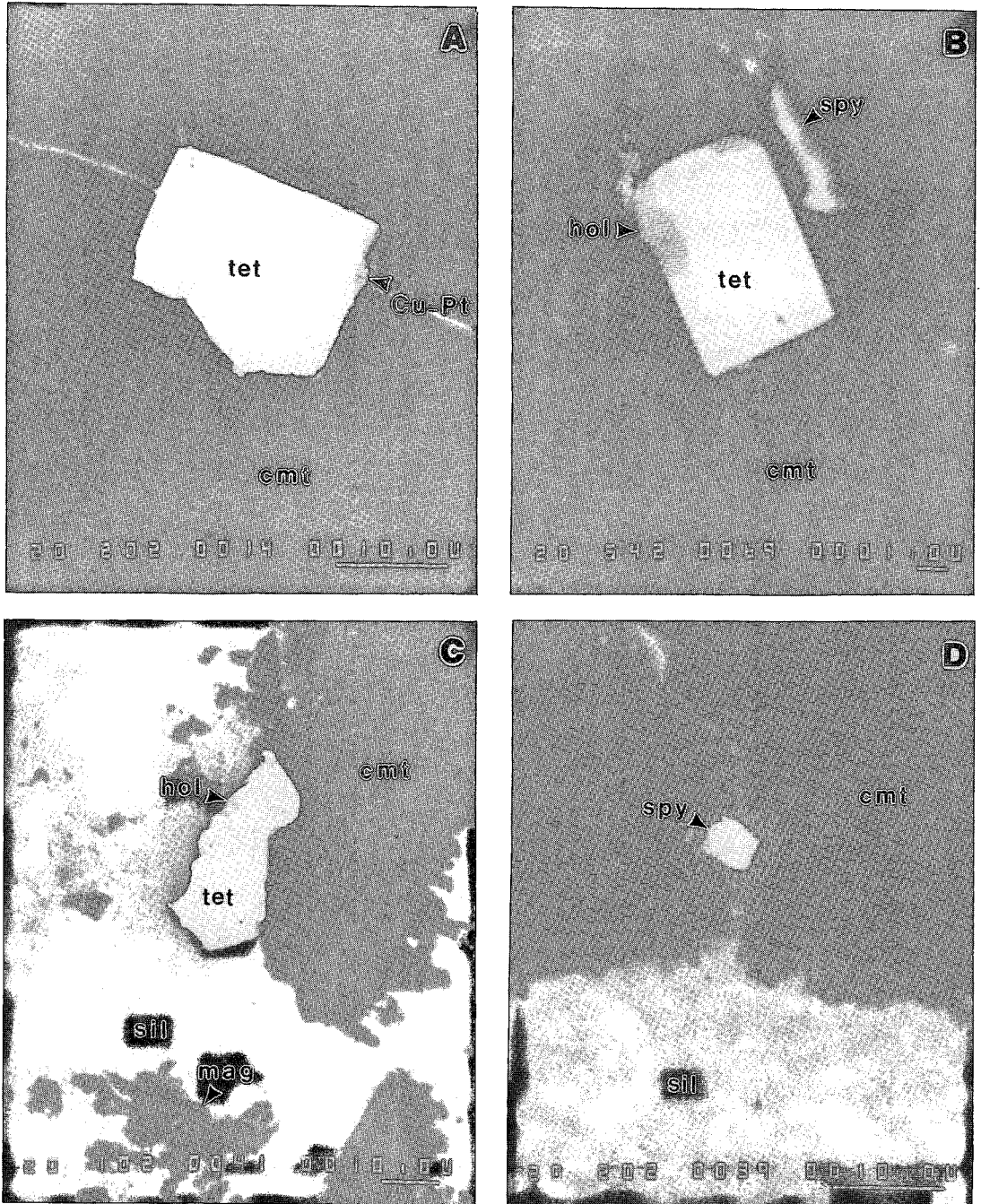


FIG. 3. Scanning electron microscope (SEM) photomicrographs of platinum-group minerals (PGM) in chromites: A. Subhedral inclusion of tetraferroplatinum(?) (tet) in chromite (cmt) with a thin, marginal zone of platinian copper (Cu-Pt) next to a fracture (GN-147B); B. Euhedral inclusion of tetraferroplatinum(?) with marginal alteration to hollingworthite (hol). Nearby sperrylite (spy) occupies a fracture in host chromite (GN87-146); C. Anhedral tetraferroplatinum(?) with hollingworthite surrounded by chromite and serpentine (sil). Lighter grey zone at margin of chromite is area of "ferritchromite"-magnetite (mag) alteration (GN87-146B); D. Subhedral inclusion of sperrylite, probably a pseudomorph after platinum alloy, straddling a fracture in chromite lined with "ferritchromite"-magnetite (GN87-146B). Bar scale = 10 μm , except in B (1 μm).

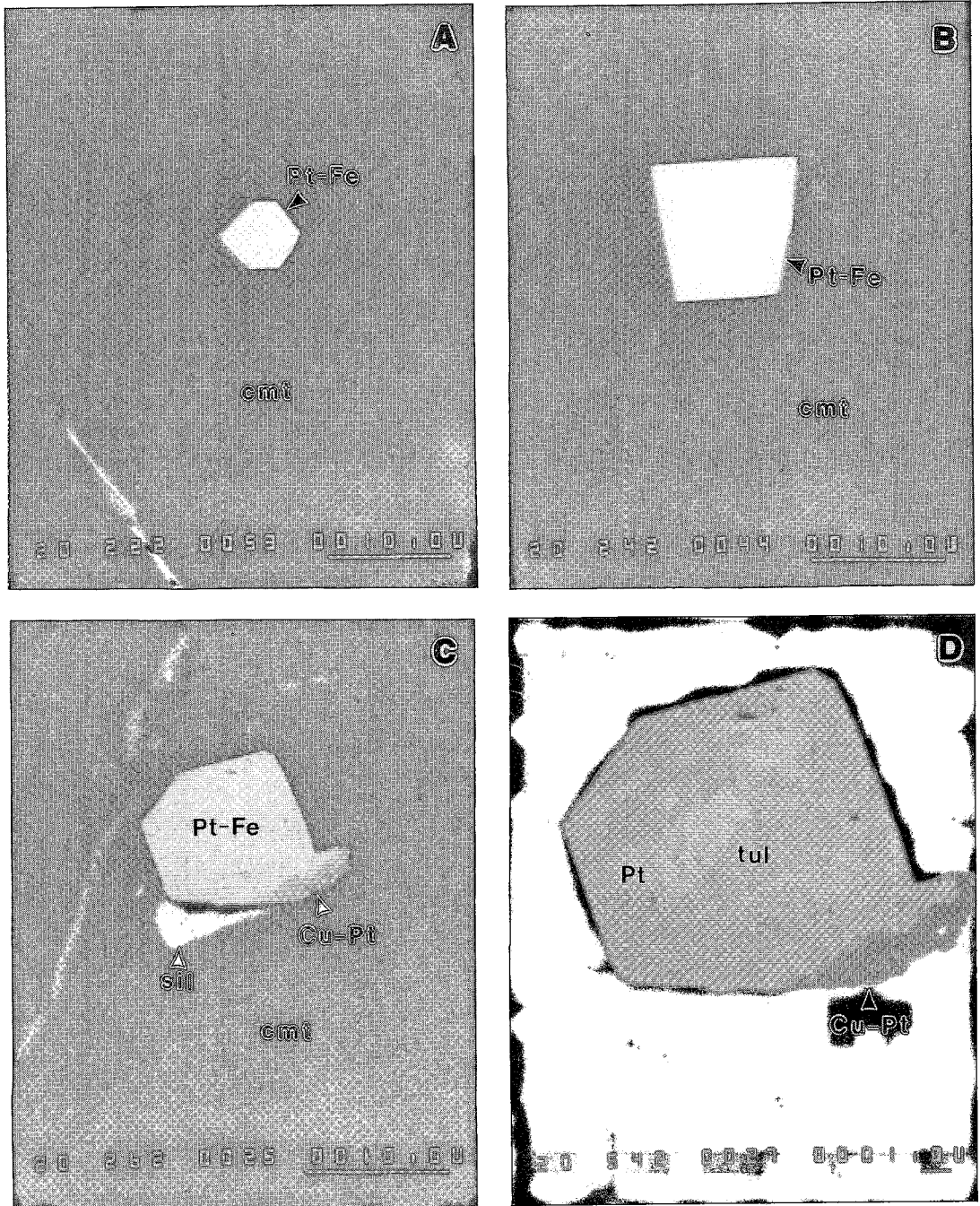


FIG. 4. SEM photomicrographs of Pt-Fe alloys in chromitites: A. Euhedral isoferroplatinum(?) inclusion in chromite (cmt) (GN87-148A); B. Euhedral isoferroplatinum(?) inclusion (GN87-146B); C. Euhedral composite Pt-Fe alloy with peripheral replacement by platinian copper (Cu-Pt) and attached euhedral Mg-rich chlorite (sil) (GN87-146B); D. Magnification of C showing irregular intergrowth of tulameenite(?) (tul), isoferroplatinum(?) (Pt) and platinian copper (Cu-Pt). Bar scale = 10 μm , except in D (1 μm).

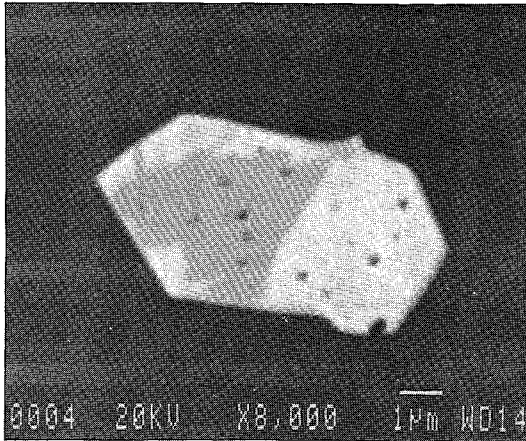


FIG. 5. SEM image of two attached euhedral crystals of platinum alloy hosted by chromite (black) in Tulameen chromitite. Larger crystal exhibits a core of "tetraferroplatinum" (dark grey) and rim of "isoferroplatinum" (white) in irregular contact with core. Smaller crystal seems to consist entirely of "isoferroplatinum", probably because the plane of the section traverses the rim of this crystal (*cf.* analyses 2 and 13, Table 2A).

systematically below detection limits. The atomic proportions of ΣPGE (49.7–52.5%) extend to the composition of a grain of ferroan platinum ($\Sigma PGE = 52.5\%$) in Similkameen placers (grain no. 9, Table 2, Cabri & Feather 1975). However, platinum alloys in the chromitites contain twice as much Cu and an order of magnitude more Ni than ferroan platinum in the placers.

Slight differences are observed among "tetraferroplatinum" compositions from different chromitites. For example, alloy grains in GN87-147 form a tight grouping in most plots (Fig. 6) and are distinguished by a greater abundance of Ir and marginally higher Fe than stoichiometrically similar grains of alloy in chromitite GN87-146 (Table 2A).

Grains of platinum alloy whose compositions lie nearer $Pt_{2.5}(Fe, Ni, Cu)_{1.5}$ (60.5–65.6 at.% ΣPGE) are tentatively assigned to "isoferroplatinum", ideally Pt_3Fe . They contain small amounts of Pd, Rh and Ir (up to 3.6 wt.%), and one grain carries Os, whereas Ru and Sb are routinely below detection limits (Table 2A). Absolute abundances of Ni and Cu are consistently lower in "isoferroplatinum" than in "tetraferroplatinum" (Table 2A, Figs. 6B, C), and Ni/Cu ratios are slightly higher in the former species (2.6 *versus* 1.7 at.%, respectively).

The majority of the grains of alloy seem to be homogeneous in composition. Rarely, coexisting alloys of $Pt(Fe, Ni, Cu)$ and $Pt_{2.5}(Fe, Ni, Cu)_{1.5}$ are found within a single grain (Table 2A, analyses 2-13 and 4-16; Fig. 6). In one case, a euhedral crystal locked in chromite exhibits a core of "tetraferroplati-

num" surrounded by an irregular rim of "isoferroplatinum" (Fig. 5). As discussed later, this rim may result from a high-temperature subsolidus reaction rather than a magmatic overgrowth formed prior to incorporation within chromite. Grains of relatively Ni- and Cu-free alloy of " Pt_2Fe " bulk composition were reported by Johan *et al.* (1989) from primary mineralization in Alaskan-type intrusions near Fifield, Australia. The latter grains, however, comprise fine heterogeneous intergrowths of Pt_3Fe and $PtFe$ that were accounted for by cooling within the miscibility gap in this part of the system Pt-Fe (*cf.* Cabri & Feather 1975).

Grains of platinum alloy with appreciable Fe and Cu (and Sb in analysis 18, Table 2A), and formulae that may be expressed as $Pt_2(Fe, Cu, Ni, Sb)_2$, are tentatively assigned to *tulameenite* (Pt_2FeCu). The antimony-rich grain contains 6.9 wt.% Sb *versus* a maximum of 5.0 wt.% Sb in previously published analyses of *tulameenite* (Cabri *et al.* 1973, Cabri & Hey 1974). Minor substitution of Rh, Pd, Ir and Os occurs for Pt. One composition falls on the Pt_2FeCu - Pt_2NiFe tie line; the other plots within the Pt_2FeCu - Pt_2CuNi - Pt_2Cu_2 triangle (Fig. 6D). Locally, *tulameenite*(?), accompanied by platinian copper, forms complex intergrowths with "isoferroplatinum" and has partly replaced the primary euhedral grain of Pt-Fe-Ni-Cu alloy (analysis 15, Table 2A; Figs. 4C, D).

Geversite ($PtSb_2$) is hosted by either chromite or serpentine, and locally occurs at chromite-serpentine contacts, where it forms anhedral intergrowths with other *PGM* (excluding Pt-Fe-Ni-Cu alloys) and base-metal sulfides, arsenides and antimonides. *Geversite* has been identified in fractures accompanied by serpentine and carbonate (Figs. 7A, B) and may form relict cores of compound grains surrounded by breithauptite (Fig. 7C), platinum oxide (Fig. 7D), or platinian copper and hollingworthite (Fig. 8A). Rarely, *geversite* occurs as subhedral inclusions in chromite that may represent a pseudomorph after a Pt-Fe-Ni-Cu alloy (Fig. 7B). One relatively large (30 μm) grain of *geversite* contains inclusions of irarsite. Microprobe analyses (Table 3) confirm the presence of Rh, Ir, Fe, Cu, Ni and As as minor constituents; in addition, Pd and Ru were reported by St. Louis *et al.* (1986).

Minerals of the *hollingworthite-irarsite* ($RhAsS$ - $IrAsS$) solid-solution series also are fairly common. *Hollingworthite*, associated with sperrylite, replaces the rim of platinum alloy grains in fractured chromite (Figs. 3B, C). *Hollingworthite* and *irarsite* also form a minor constituent of composite intergrowths of *geversite*, *breithauptite*, platinian copper, platinum oxide, and nickel arsenides and sulfides (Fig. 8A). Small quantities of Pt, Sb, Cu and Ni were detected by qualitative energy-dispersion analysis, but owing to the small grain-size, we cannot rule out

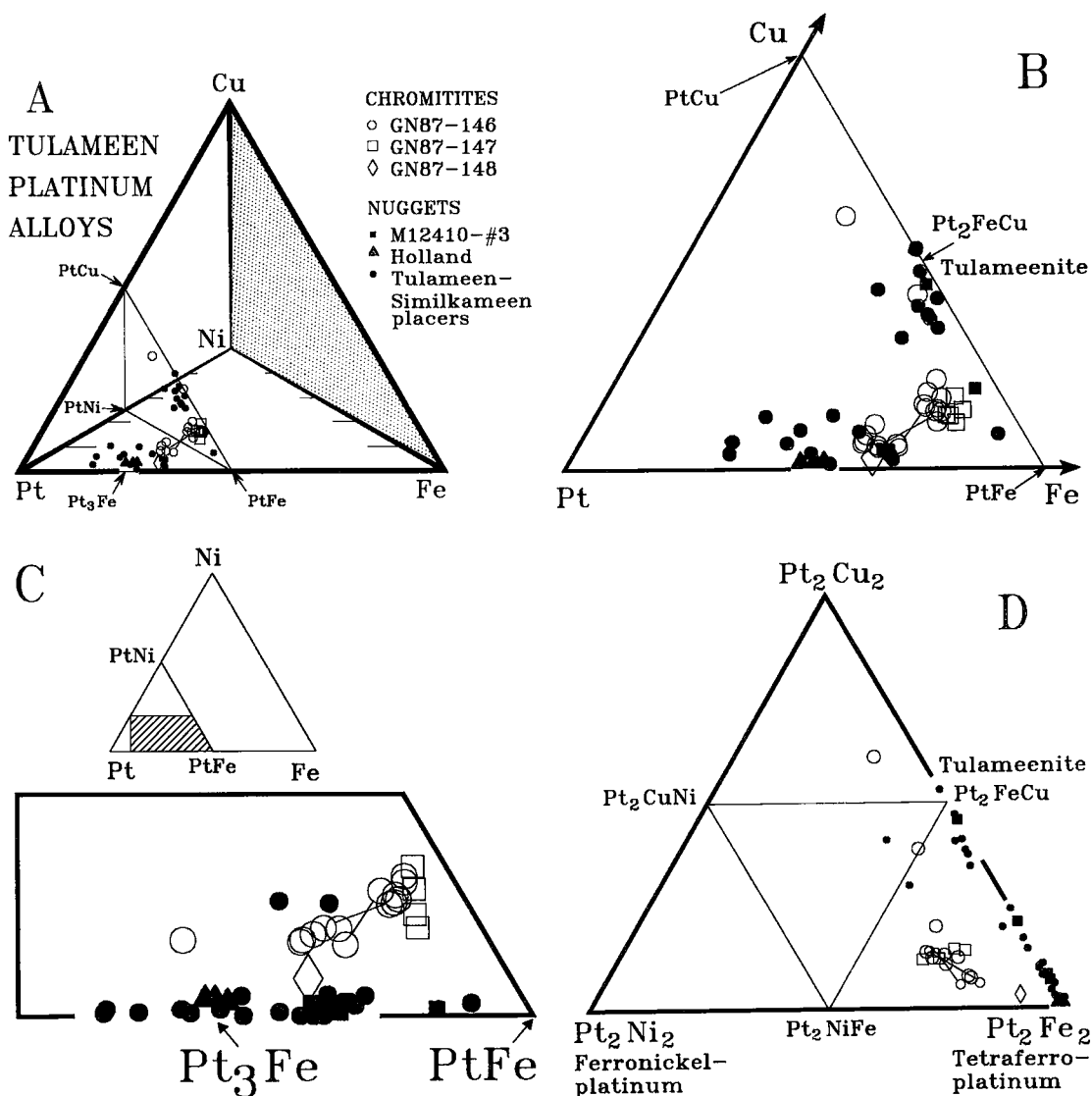


FIG. 6. Plots of compositions of platinum alloys (atom %) that occur in Tulameen chromitites and placer nuggets. A. Alloys plotted in the Pt-Fe-Cu-Ni tetrahedron, showing ideal compositions of isoferroplatinum (Pt_3Fe) and tetraferroplatinum ($PtFe$). B. Cu-Pt-Fe projection of alloy compositions onto the face of the tetrahedron. C. Ni-Pt-Fe projection onto base of tetrahedron. D. Pt_2Fe_2 - Pt_2Cu_2 - Pt_2Ni_2 equivalent plot of alloy compositions projected onto the PtFe-PtCu-PtNi plane in the tetrahedron (shown in A). Note that isoferroplatinum and tetraferroplatinum occupy the same point in this projection. Tie lines connect coexisting alloys (analyses 2-13 and 4-16, Table 2A). Compositional data for Tulameen-Similkameen placer grains taken from Cabri *et al.* (1973, Table 1), Cabri & Hey (1974, Table 1), and Cabri & Feather (1975, Table 2). For purposes of these plots, all platinum-group elements are included with Pt.

contributions arising from secondary fluorescence of surrounding minerals.

Sperrylite ($PtAs_2$) also is found as a fracture filling, along with serpentine, carbonate, and rare holdingworthite (Fig. 3B). A subhedral crystal of sperrylite lying on a fracture in chromite appears to be

completely enveloped by a "ferritchromite"-magnetite alteration zone (Fig. 3D). This situation is analogous to the one involving geversite (Fig. 7B) and may likewise represent replacement of a grain of primary Pt-Fe-Ni-Cu alloy. Minor amounts of Ru, Fe, Sb and S identified by qualitative energy-

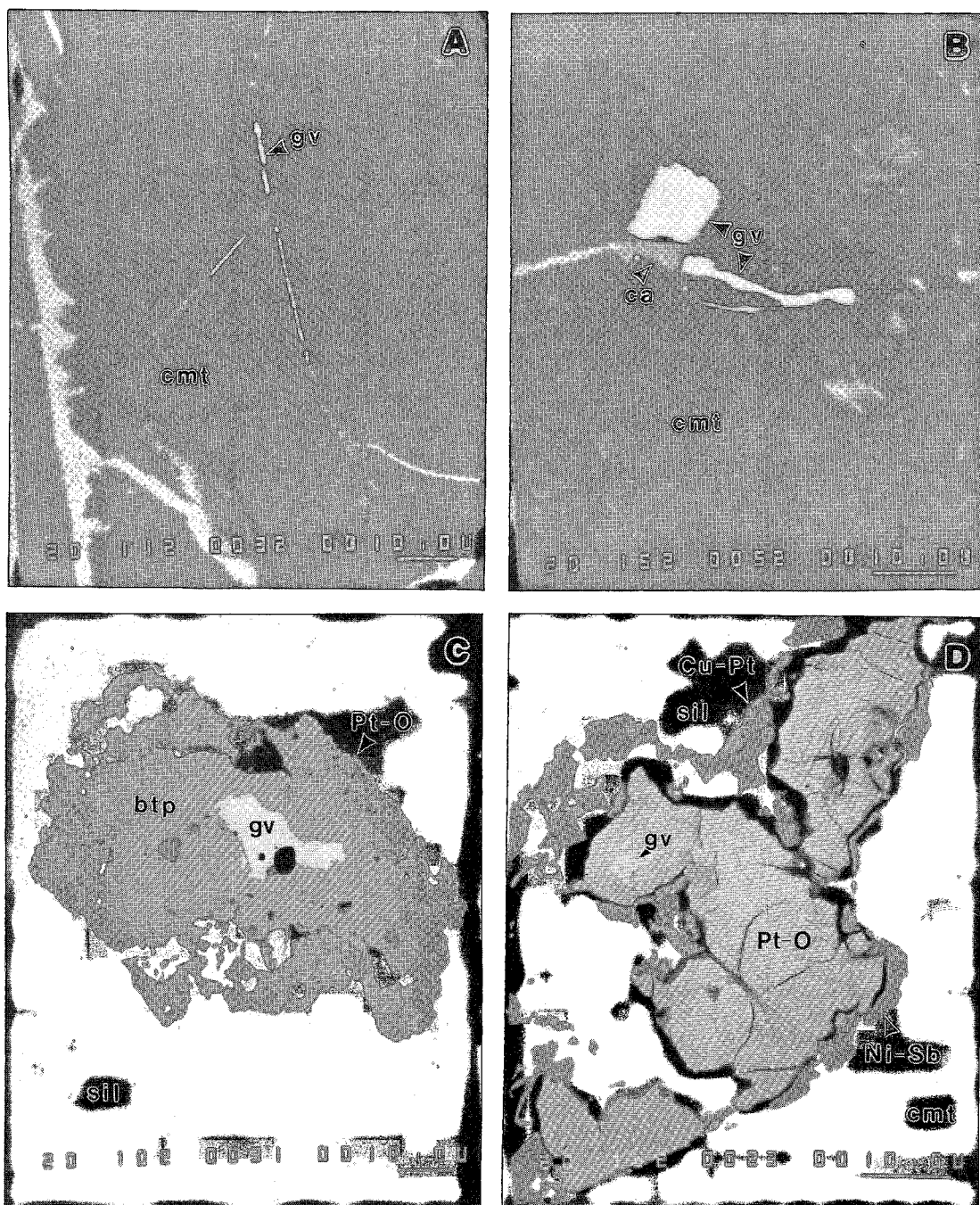


FIG. 7. SEM photomicrographs of PGM in fractures and complex polymineralic intergrowths in chromitite: A. Fractures in chromite (cmt) filled by serpentine (black) and a Pt antimonide, probably geversite (gv). Note alteration of chromite to "ferritchromite"-magnetite (medium grey) along wide fractures at left (GN87-148); B. Fissure in chromite filled by geversite (gv) and calcite (ca) adjacent to subhedral geversite grain, probably a pseudomorph after primary platinum alloy in chromite (GN87-148A); C. Compound zoned grain of geversite and breithauptite (btp) with a Pt oxide rim enclosed in serpentine (GN87-148A); D. Composite grain of predominantly Pt oxide with relic geversite enclosed in a vein of serpentine in chromite. Thin discontinuous rims of platinumian copper (Cu-Pt) and a nickel antimonide (Ni-Sb), probably breithauptite, also are present (GN87-148B). Bar scale = 10 μm .

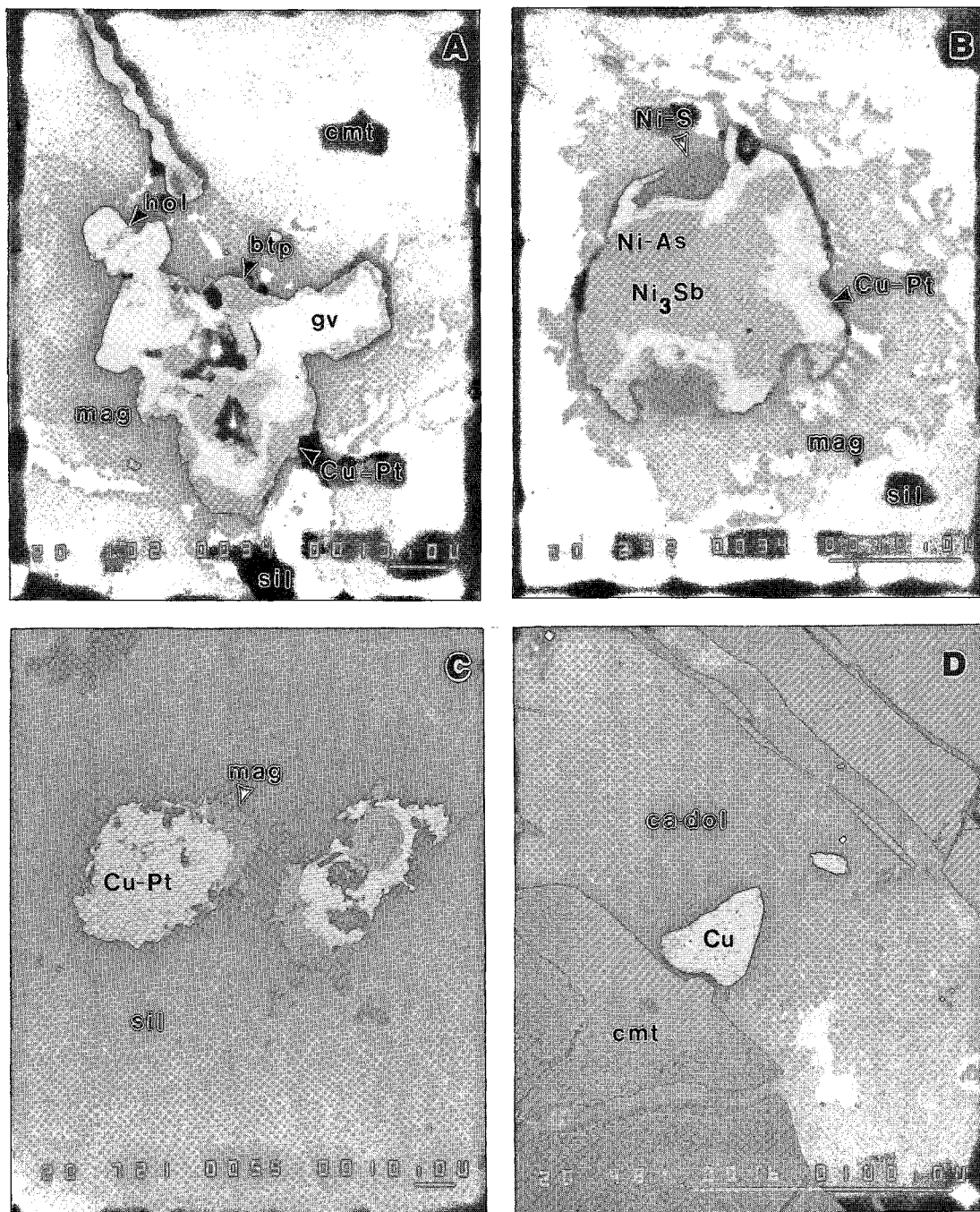


FIG. 8. SEM photomicrographs of complex mineral intergrowths: A. Large altered grain exhibiting a core of geversite (gv) surrounded by irregular intergrowths of breithauptite (btp), platnian copper (Cu-Pt) and hollingworthite (hol) filling an irregular fissure in chromite (cmt) that is marginally altered to "ferritchromite"-magnetite (mag) (GN87-146A); B. Complex intergrowth of platnian copper, nickel antimonide (Ni_3Sb), nickel arsenide (Ni-As) and nickel sulfide (Ni-S) enclosed by serpentine and magnetite (GN87-148A); C. Intergrowth of magnetite - platnian copper in serpentine (GN87-148A); D. Two anhedral grains of native copper (Cu) in a carbonate-filled (ca-dol) fracture in chromite (GN87-147B). Bar scale = 10 μm , except in D (100 μm).

TABLE 3. ELECTRON-MICROPROBE DATA ON GEVERSITE IN CHROMITITE

Anal. No.	Grain Size (μm)	Weight per cent								Atomic proportions										
		Pt	Rh	Ir	Fe	Cu	Ni	Sb	As	Total	Pt	Rh	Ir	Fe	Cu	Ni	Sum	Sb	As	Sum
1	10 x 25	42.9	n.d.	n.d.	0.80	0.25	0.22	54.9	1.2	100.27	0.93			0.06	0.02	0.01	1.02	1.91	0.07	1.98
2	8 x 10	41.4	0.24	0.14	0.92	n.d.	n.d.	55.5	0.28	98.48	0.92	0.01	<0.01	0.07			1.00	1.98	0.02	2.00
3	8 x 15	42.9	0.18	0.42	n.d.	n.d.	0.53	55.7	n.d.	99.73	0.95	0.01	0.01			0.04	1.01	1.99		1.99

n.d. = not detected; minimum detection limits in wt. % are: Fe, Cu, Ni 0.03; Rh 0.05; As, Ir 0.10.

1. GN87-146A: complex polyminerale grain with platinian copper, Ni antimonide and hollingworthite enclosed in magnetite-chromite.

2. GN87-148A: in contact with calcite-dolomite.

3. GN87-148A: in breithauptite with Pt oxide enclosed in serpentine.

TABLE 4. ELECTRON-MICROPROBE DATA ON PLATINIAN COPPER IN CHROMITITE AND PLACER NUGGETS

Anal. No.	Grain Size (μm)	Weight per cent									Atomic proportions							
		Pt	Rh	Pd	Ir	Cu	Fe	Ni	Sb	Totals	Pt	Rh	Pd	Ir	Cu	Fe	Ni	Sb
1	13x30	33.0	0.10	0.07	-	65.6	0.17	0.40	0.15	99.49	0.14	<0.01	<0.01		0.85	<0.01	0.01	<0.01
2	8x40	34.9	0.10	0.05	-	61.9	0.59	0.29	1.3	99.13	0.15	<0.01	<0.01		0.83	0.01	<0.01	0.01
3	3x8	34.3	0.14	0.08	-	60.9	1.2	0.78	1.7	99.10	0.15	<0.01	<0.01		0.81	0.02	0.01	0.01
4	15x40	36.5	0.10	0.05	-	60.9	0.37	0.69	0.68	99.29	0.16	<0.01	<0.01		0.82	0.01	0.01	<0.01
5	10x18	30.4	0.09	0.08	-	59.2	2.1	3.7	3.2	98.77	0.13	<0.01	<0.01		0.77	0.03	0.05	0.02
6	10x25	40.1	0.85	0.18	8.6	48.0	2.5	0.07	n.d.	100.30	0.19	0.01	<0.01	0.04	0.71	0.04	<0.01	
7	10x25	42.9	0.57	0.24	5.6	48.2	2.2	0.07	n.d.	99.78	0.21	<0.01	<0.01	0.03	0.72	0.04	<0.01	
8	10x25	41.8	n.d.	0.30	n.d.	57.3	0.54	n.d.	n.d.	99.94	0.19		<0.01		0.80	0.01		
9	5x80	44.7	n.d.	0.45	n.d.	53.7	0.66	n.d.	n.d.	99.51	0.21		<0.01		0.78	0.01		
10	5x80	39.8	0.10	0.36	0.40	58.1	0.64	n.d.	n.d.	99.40	0.18	<0.01	<0.01	<0.01	0.80	0.01		

1. GN87-148A: in serpentine; 2. GN87-148B: with Pt oxide, geversite, serpentine and chromite; 3. GN87-148B: with Ni-antimonide and irarsite in chromite; 4. GN87-148A: with magnetite in serpentine; 5. GN87-146: with Ni-arsenide in serpentine(?) between chromite grains; 6 - 8. M12410, nugget #3: 10 micrometer-wide ring-shaped inclusion in tulameenite; 9 and 10. M12410, nugget #3: as veinlets in tulameenite. n.d. = not detected; - = not determined.

TABLE 5. ELECTRON-MICROPROBE DATA ON PLATINUM OXIDE(?) IN CHROMITITE

Weight per cent								
Pt	Rh	Ir	Fe	Cu	Ni	Sb	O*	Total
78.7	0.28	0.92	0.33	4.1	4.4	2.6	8.67	100.00
76.2-80.3**		0.59-1.3		3.5-4.7	3.0-5.5	2.1-3.0		

* Oxygen by difference. ** Range.

GN87-148B: complex multiminerale grain with platinian copper, nickel antimonide, geversite(?) and nickel oxide, and surrounded by serpentine, magnetite, and chromite.

dispersion analysis may also be due to secondary fluorescence of neighboring minerals. Similar compositions were obtained by St. Louis *et al.* (1986), who found sperrylite to be one of the most abundant PGM in the Grasshopper Mountain chromitites.

Platinian copper forms a minor phase that occurs late in the paragenetic sequence. It contains up to 36.5 wt.% Pt and small quantities of Fe (≤ 2.1 wt.%), Ni (≤ 3.7 wt.%), Sb (≤ 3.2 wt.%), Rh and Pd (< 0.15 wt.% each; Table 4). This Cu-Pt alloy replaces parts of the rim of euhedral grains of platinum alloys in fractured chromite crystals (Figs. 3A, 4C, D), occurs as a thin discontinuous overgrowth on composite Pt oxide - geversite grains (Figs. 7D, 8A), and forms intergrowths with magnetite and nickel sulfides, arsenides and antimonides (Figs. 8B, C). A Cu-Pt alloy with up to 33 wt.% Pt has been

reported previously from the Thetford Mines (Corrivaux & Laflamme 1990) and Shetland ophiolites (Prichard *et al.* 1986), where it also is associated with PGM-bearing chromitites.

Among the less abundant PGM are single grains of *erlichmanite* (OsS_2) and *laurite* (RuS_2), and an undefined *platinum oxide*, which forms the largest PGM grain observed to date (150 μm). The latter phase occurs within a serpentine-filled fissure in chromite and is associated with antimonides, nickel oxide(?) and platinian copper, and locally rims breithauptite (Figs. 7C, D). Its composition is somewhat heterogeneous, with minor variations in Rh, Ir, Fe (< 1.5 wt.% each) and Cu, Ni and Sb (2-5.5 wt.%; Table 5). In addition to the PGM listed above, St. Louis *et al.* (1986) reported *native platinum* (Pt-Fe alloy, < 20 at.% Fe), *stumpflite* (PtSb), and the very rare mineral *genkinite* $[(\text{Pt}, \text{Pd})_4\text{Sb}_3]$, as determined by qualitative energy-dispersion analyses.

Base-metal minerals

Base-metal sulfides, arsenides and antimonides, and native metals and metal oxides form a minor yet persistent mineral assemblage in partly serpentinized dunites and chromitites. These minerals typically occupy veinlets or interstices between chromite grains, textures similar to those described by St.

TABLE 6. ELECTRON-MICROPROBE DATA ON THREE Ni-Sb MINERALS IN CHROMITITE

Anal. No.	Grain Size (μm)	Weight per cent								Atomic proportions							
		Ni	Cu	Fe	Ir	Pt	Rh	Sb	Total	Ni	Cu	Fe	Ir	Pt	Rh	Sum	Sb
1	5 x 20	31.1	11.8	0.90	7.0	0.24	0.79	47.8	99.63	1.36	0.48	0.04	0.09	<0.01	0.02	1.99	1.01
2	30 x 60	31.1	0.32	n.d.	n.d.	1.7	0.14	65.9	99.16	0.97	0.01		0.02	<0.01	1.00	1.00	
3	7 x 12	57.6	0.26	0.66	n.d.	n.d.	n.d.	40.5	99.02	2.95	0.01	0.04			3.00	1.00	

n.d. = not detected; minimum detection limits in wt. % are: Fe 0.03; Rh 0.05; Ir, Pt, As 0.10; As was not detected.

- GN87-148B: undetermined (Ni, Cu)₂Sb mineral complexly intergrown with platinum copper and irarsite enclosed in chromite.
- GN87-148A: breithauptite in complex polyminerale grain with geversite and Pt oxide enclosed in serpentine.
- GN87-148A: undetermined Ni₃Sb mineral in complex polyminerale grain with platinum copper, undetermined Ni arsenide and sulfide, surrounded by magnetite which is enclosed in serpentine.

TABLE 7. ELECTRON-MICROPROBE DATA ON AN UNUSUAL NI ARSENIDE IN CHROMITITE

Anal. No.	Grain Size (μm)	Weight per cent							Atomic proportions						
		Ni	Cu	Fe	As	Sb	Total	Ni	Cu	Fe	Sum	As	Sb	Sum	
1	5 x 8	58.8	0.22	4.1	33.3	3.2	99.62	6.47	0.02	0.47	6.96	2.87	0.17	3.04	
2	10 x 23	60.8	0.37	1.5	34.3	1.9	98.87	6.72	0.04	0.17	6.93	2.97	0.10	3.07	

- GN87-146A: complex polyminerale grain with platinum copper, Ni sulfide and small Pt-Fe alloy grain in magnetite.
- GN87-146B: complex polyminerale grain with undetermined Ni antimonide, platinum copper and geversite enclosed in magnetite-chromite.

Louis *et al.* (1986) (Figs. 7C, D, 8A, B). The most widespread sulfide mineral is disseminated pyrite. Nickel sulfides include *millerite* or *heazlewoodite*, and an undetermined Ni-Co-Fe sulfide intergrown with "ferritchromite"—magnetite and serpentine. Other Ni-bearing sulfides identified by St. Louis *et al.* (1986) are *pentlandite*, *violarite*, and *bravoite*. Compositions of three Ni-Sb minerals, including *breithauptite*, are given in Table 6. They contain small quantities of Pt (≤ 1.7 wt. %), Rh (≤ 0.79 wt. %) and Ir (up to 7.0 wt. %) in addition to Cu (≤ 11.8 wt. %) and Fe (≤ 0.9 wt. %). Nickel arsenides include *maucherite*(?) and *Ni₇As₃* that contains minor Cu, Fe and Sb (Table 7). Native metal and oxide phases include *native copper*, identified in Ca-Mg carbonate veinlets (Fig. 8D), *native silver*, and *copper and nickel oxides*.

PETROGRAPHY AND MINERALOGY OF PLACER NUGGETS

Aspects of the mineralogy of placer nuggets in the Tulameen-Similkameen rivers and their tributaries, and the PGM in particular, have been documented previously (Cabri *et al.* 1973, Harris & Cabri 1973, Cabri & Hey 1974, Cabri & Feather 1975, Raicevic & Cabri 1976). Descriptions of specific nuggets given below augment these earlier observations. Results of electron-microprobe analysis of platinum alloys are given in Table 2B and plotted in Figure 6.

Holland nugget

The Holland nugget, 4.5 mm in diameter, is a

rounded specimen comprising cumulus chromite and minor olivine (< 1 mm) set in a matrix of Pt-Fe alloy, probably isoferroplatinum, which contains up to 2.3 wt. % Pd (Table 2B; Figs. 6, 9A; see also Raicevic & Cabri 1976, Fig. 3). A single grain of laurite (0.5 mm) is included within the alloy. Iridosmine, Pt oxide and very fine intergrowths of tolovkite (IrSbS), geversite, sperrylite, pentlandite(?) and an undetermined Pd-Sb mineral also were observed. The few crystals of olivine that are present occur at the rim of the nugget. Chromite forms euhedral to subhedral grains in which the internal fractures and rims are altered to magnetite. The latter mineral also forms very fine grained intergrowths in Pt-Fe alloy. The ratio of chromite + olivine to PGM is approximately 1:1. Serpentine and Mg-rich chlorite are trace constituents.

Lincoln nugget

The Lincoln nugget (3 x 5 mm) also contains euhedral to subhedral cumulate chromite and olivine, and intercumulate Pt-Fe alloy, probably isoferroplatinum. Thin zones of magnetite separate the chromite crystals from the platinum alloy, which contains relatively coarse intergrowths of magnetite that are particularly well developed adjacent to chromite (Fig. 9B; see also Raicevic & Cabri 1976, Fig. 4). Inclusions of laurite and euhedral chlorite, possibly pseudomorphous after phlogopite, also are observed (Figs. 9B-D). A single lath of iridosmine (25 x 100 μm) in Pt-Fe alloy was reported by Harris & Cabri (1973), and a few small inclusions of genkinite also were observed (not reported previ-

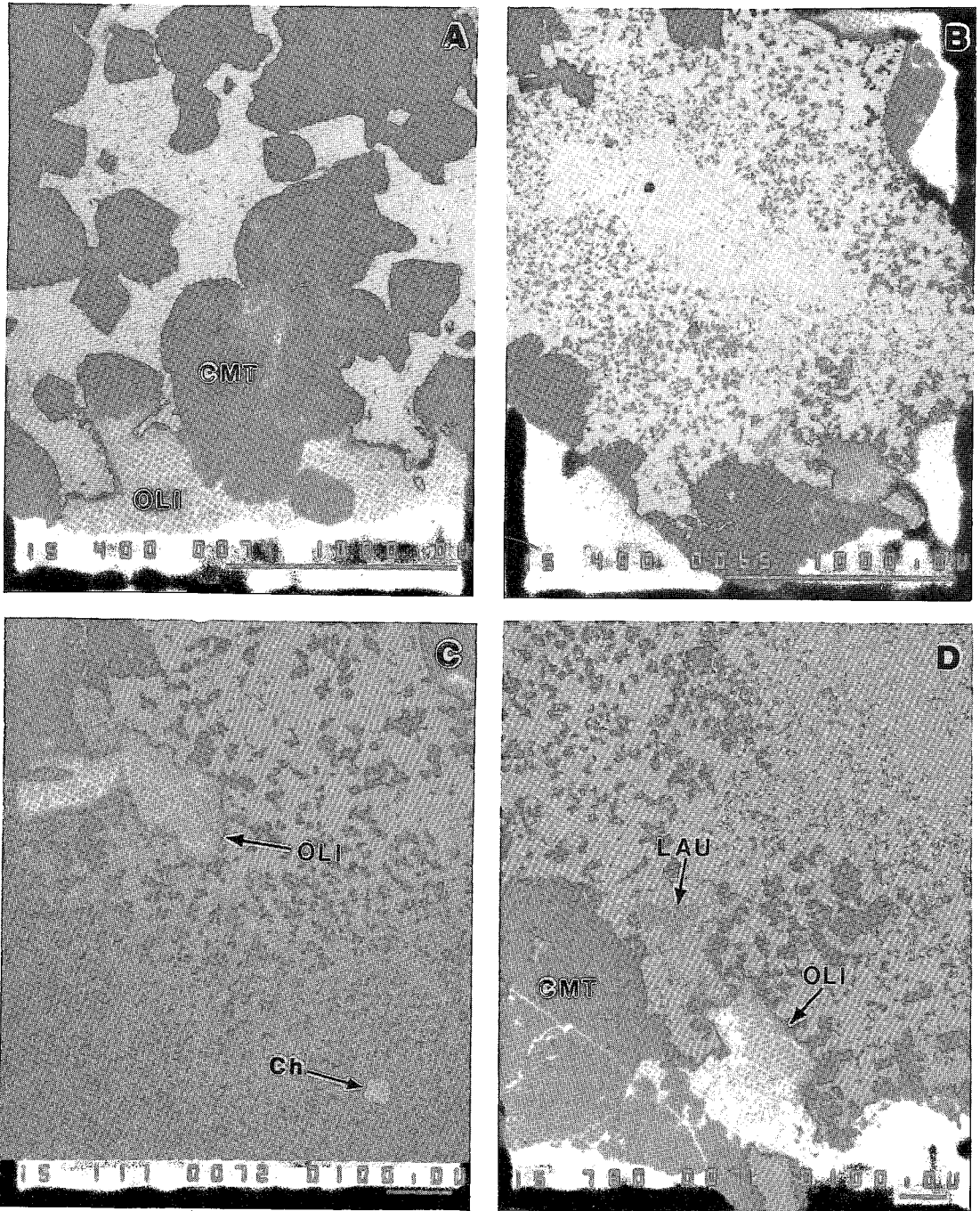


FIG. 9. SEM photomicrographs of Holland and Lincoln nuggets. All of the chromite, in both nuggets, has a thin rim of magnetite of variable thickness (10–25 μm) that cannot readily be seen on these photomicrographs. A. Subhedral chromite (cmt) and minor olivine (oli) included in Pt-Fe alloy (white) containing fine intergrowths of magnetite (Holland nugget); B. Pt-Fe alloy (white) with irregular intergrowths of magnetite bordered by chromite and olivine (Lincoln nugget); C. Enlargement of B showing olivine inclusion (oli), euhedral grain of chlorite (ch) and magnetite intergrowths in Pt-Fe alloy; D. Enlargement of B showing an inclusion of laurite (L) in Pt-Fe alloy near the contact with chromite-olivine. Bar scale = 1 mm in A–B, 100 μm in C–D.

TABLE 8. ELECTRON-MICROPROBE DATA ON MAGNETITE IN PLATINUM NUGGETS

Anal. No.	1	2	3	4	5
SiO ₂	-	-	0.26	0.27	-
TiO ₂	-	-	-	-	-
Al ₂ O ₃	-	-	-	-	-
Cr ₂ O ₃	0.86**	0.63**	-	-	1.2**
Fe ₂ O ₃ *	68.3	68.2	68.4	68.6	67.8
FeO	28.5	28.3	28.7	28.2	28.8
MnO	-	0.18	0.18	0.25	0.30
MgO	1.5	1.4	1.4	1.7	1.1
Total	99.16	98.71	98.94	99.02	99.20
Cations per 32 Oxygen atoms					
Si			0.080	0.083	
Ti					
Al					
Cr					0.292
Fe ³⁺	15.791	15.846	15.840	15.834	15.708
Fe ²⁺	7.313	7.309	7.390	7.240	7.417
Mn		0.047	0.047	0.065	0.078
Mg	0.687	0.644	0.643	0.778	0.505

* Calculated assuming ideal stoichiometry.

** Part of the Cr₂O₃ reported could be due to fluorescence from the surrounding chromite.

- = not determined.

1-2: Lincoln nugget, magnetite rim on chromite;

3-4: Lincoln nugget, magnetite intergrowth in Pt-Fe alloy;

5: Holland nugget, magnetite rim on chromite.

ously). Oxide alteration products of chromite are identical in composition to the magnetite intergrowths in Pt-Fe alloy (Table 8).

M12410 nuggets

Nugget 1 is a medium-size (3 × 4 mm) specimen comprising mainly Pt-Fe alloy (isoferroplatinum?) carrying generally fine-grained intergrowths of osmiridium (<5 to 20 × 20 μm), very thin laths of iridosmine, and minor laurite (Fig. 10). Chromite is a subordinate constituent, forming subhedral to euhedral crystals and grain aggregates (<1 mm). Magnetite forms an intergrowth with Pt-Fe alloy and is a persistent alteration product of chromite. This nugget is particularly well endowed with a diverse assemblage of primary and secondary silicate inclusions (Fig. 10D; described below).

Nugget 2 is the smallest (2 × 4 mm) of the three nuggets. It consists of Pt-Fe alloy (probably isoferroplatinum) with numerous fine-grained intergrowths of osmiridium, generally <5 μm in size, but reaching 20 × 100 μm. Chromite (<1 mm) is a minor constituent and locally exhibits euhedral margins rimmed by magnetite. No silicate minerals were observed.

Nugget 3 is the largest specimen (4 × 7 mm) and comprises approximately 50 vol.% of subhedral chromite embedded in a matrix of platinum alloy, comprising principally tulameenite with minor isoferroplatinum(?) [Pt_{2,6}(Fe,Cu,Ni)_{1,4}] and rare tetraferroplatinum(?) [Pt(Fe,Cu,Ni), Fig. 11]. The latter two alloys contain approximately 0.9 and 4.6 wt.% Cu,

respectively, and similar amounts of Ir (6.5–7.0 wt.%; Table 2B, Fig. 6). Other PGM include fine-grained osmiridium (generally <5 μm in size, but reaching 30 × 40 μm) and thin laths of iridosmine set in platinum alloy. In addition, platinum copper with up to 44.7 wt.% Pt and 8.6 wt.% Ir is intergrown with magnetite and forms veinlets within, and rims around, tulameenite (Table 4; Fig. 11D). Subhedral cumulate olivine and a variety of other silicate minerals enclosed in chromite and platinum alloy also have been identified (described below).

PGM IN CHROMITITES VERSUS PLACERS

The species of PGM in chromitites and placer deposits of the Tulameen region and their relative frequency are listed in Table 9. These data represent an important first step in an evaluation of the potential source(s) of PGE mineralization in the placers.

The principal PGM in both chromitites and placer nuggets are Pt-Fe-Cu-Ni alloys. However, the most abundant alloy species in chromitites is "tetraferroplatinum" [Pt(Fe,Ni,Cu)], closely followed by "isoferroplatinum" [Pt_{2,5}(Fe,Ni,Cu)_{1,5}], whereas "isoferroplatinum" [Pt_{2,6}(Fe,Cu,Ni)_{1,4} to Pt₃Fe], native and ferroan platinum predominate in the placers (Raicevic & Cabri 1976). In addition, geverite, sperrylite and Rh-Ir sulfarsenides appear in greater abundance in the chromitites. Phases present in the placers yet apparently lacking in the chromitites include Ru-Ir-Os and Pt-Ir alloys, cooperite, tolovkite and an unnamed RhSbS mineral.

If all the analytical data for Pt-Fe-Cu-Ni alloys are considered, it is clear that there is a considerable range of solid solutions (Fig. 6). Except for a nickeloan variety of tulameenite(?), placer alloys are depleted in Ni relative to those in chromitites (Figs. 6C, D), but have a similar range of Cu abundances (Fig. 6B). "Isoferroplatinum" compositions in chromitites occupy the Pt-poor end of a continuous range of essentially Pt-Fe alloys that extend to native platinum, and a small compositional gap separates "isoferroplatinum" from "tetraferroplatinum".

The mineralogical and compositional discrepancies between the PGM in chromitites and placers are perhaps not as striking as certain differences in grain size and texture. Platinum alloys in nuggets attain millimeter-scale dimensions and poikilitically enclose large primocrysts of chromite and olivine. In contrast, grains in the chromitites rarely exceed 30 μm across and are almost invariably enclosed in chromite. We note that the larger nuggets were obtained from placers near the eastern margin of the ultramafic complex, whereas material collected further downstream typically occurs as fine flakes (-150 mesh; Raicevic & Cabri 1976). We believe that these differences are best explained by inadequate sampling or complete erosion of high-grade lode occur-

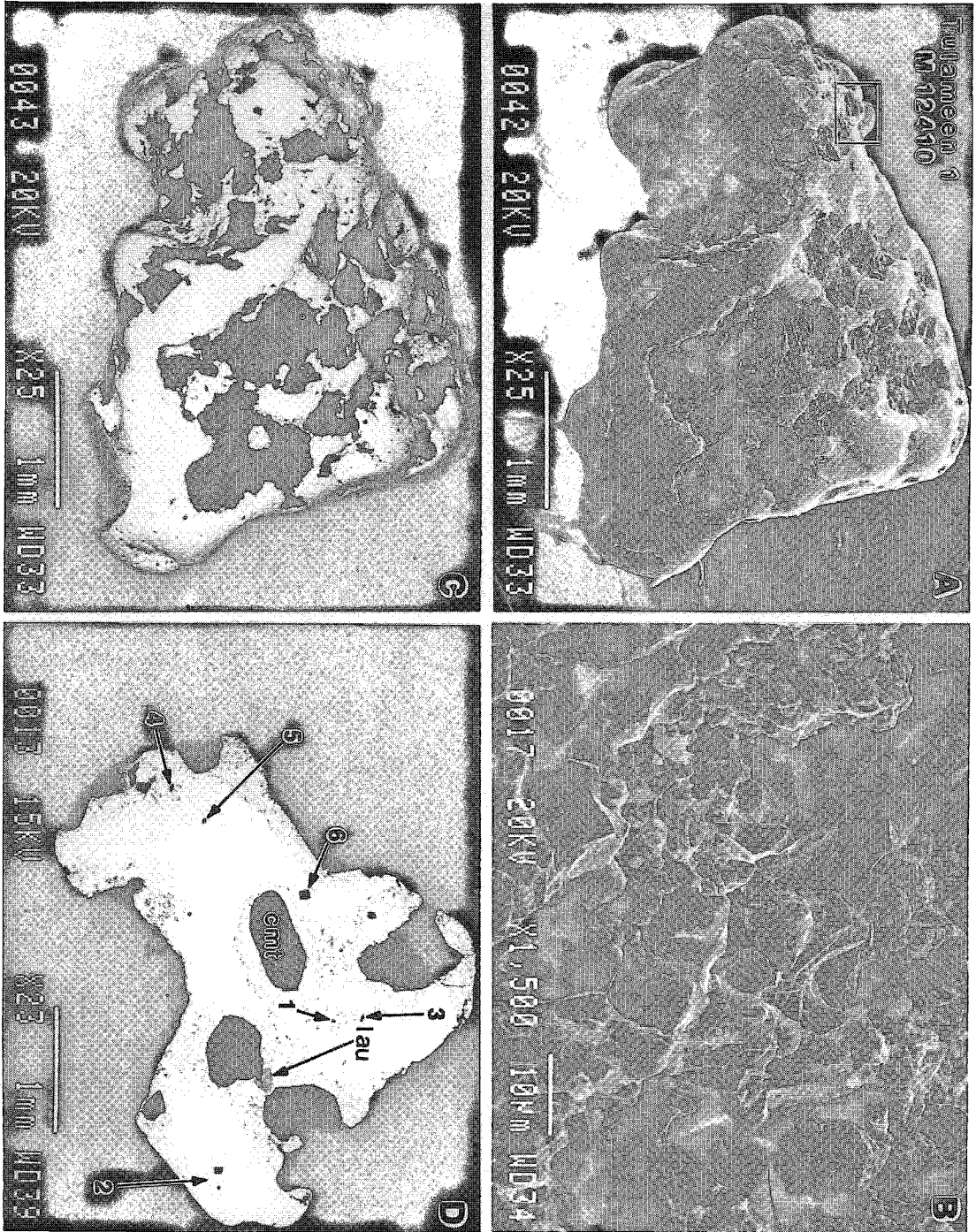


FIG. 10. SEM photomicrographs of M12410 nugget 1: A. Low-magnification image of variably pitted surface of "knobby" nugget; B. High-magnification image of area outlined in A, showing irregular surface detail of Pt-Fe alloy; C. Back-scattered electron image of A, clearly showing the chromite (dark grey) in the Pt-Fe alloy matrix (white); D. Cross section of nugget showing Pt-Fe alloy with inclusions of laurite (lau), chromite (cmt) and very fine-grained magnetite concentrated around chromite grains; arrows show the location of silicate inclusions that were analyzed (*cf.* inclusion no., Table 12, except inclusion 6, which represents an intergrowth of magnetite, chlorite and clinopyroxene). Bar scale = 1 mm, except in B (10 μ m).

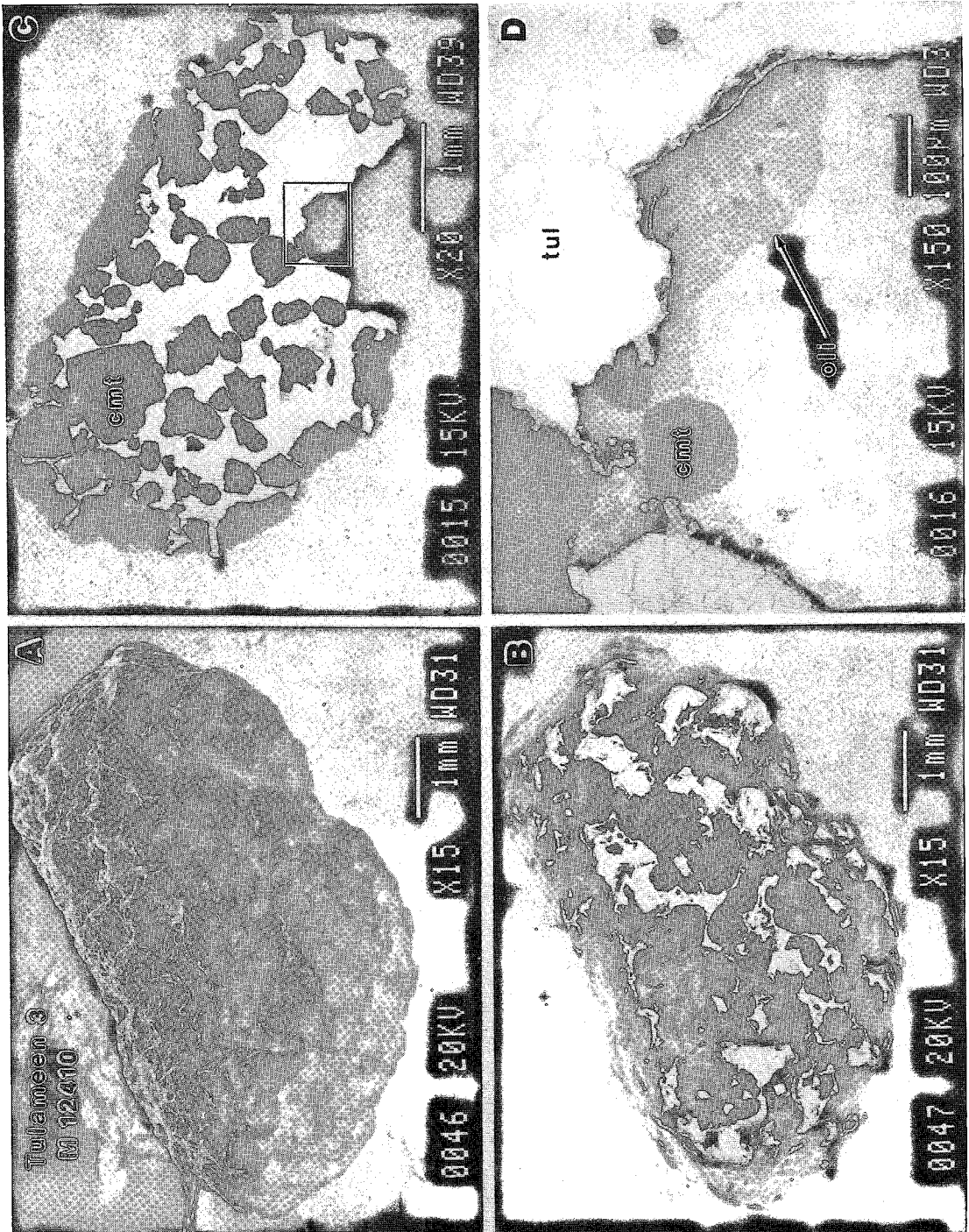


FIG. 11. SEM photomicrographs of M12410 nugget 3: A. Low-magnification image of irregular surface features of nugget; B. Back-scattered electron image, clearly distinguishing chromite (dark grey) from platinum alloy (white) comprised mainly of tulameenite, minor isoferroplatinum(?) and rare tetraferroplatinum(?); C. Cross section of nugget showing subhedral chromite (cmt) set in matrix of platinum alloy; D. Enlargement of area outlined in C showing chromite and olivine (oli) in contact with tulameenite (tul), which is veined and rimmed by platinian copper (light grey). Bar scale = 1 mm, except in D (100 μ m).

TABLE 9. PLATINUM-GROUP MINERALS IN TULAMEEN CHROMITITES AND PLACERS

Mineral	Ideal Formula	Minor Constituents	Chromitites ¹	Placers ¹	Ref. ²
cooperite	PtS	Pd,Ni	-	x	6
Cu-Pt alloy	(Cu,Pt)	Pd,Rh,Fe,Ni,Sb	xx	x	1
erlichmanite	Os ₂ S ₂	Pt,Pd,Rh,Ir	x	x	1,6
genkinite	(Pt,Pd) ₆ Sb ₃	Rh,S	x	x	1,4
geversite	PtSb ₂	Rh,Ir,Fe,Cu,Ni,As	xx	x	1,6
hollingworthite-irarsite series	Rh-Ir(AsS)	Pt,Pd,Rh,Os,Ru,Sb,Cu,Ni,Co	xx	x	1,4,6
iridium	Ir	Pd,Rh,Os,Ru,Fe,Cu,Ni	-	x	5
iridosmine	(Os,Ir)	Pt,Pd,Rh,Ru,Fe,Cu,Ni	-	xx	1,5
isoferroplatinum	Pt ₃ Fe	Pd,Rh,Ir,Os,Cu,Ni,Sb	(xxx)	xxx	1,2,6
kotulskite*	PdTe	Pt,Sb,Bi	-	x	6
laurite	RuS ₂	Rh,Ir,Os	x	x	1,6
osmiridium	(Ir,Os)	Pd,Rh,Ru,Fe,Cu,Ni	-	x	1,5
osmium	Os	Pt,Pd,Rh,Ir,Ru,Fe,Cu,Ni	-	xx	5
platiniridium	(Ir,Pt)	Os,Ru,Fe,Cu,Ni	-	x	7
platinum, ferroan	(Pt,Fe) > 20 at. % Fe	Ir,Cu,Ni	-	xxx	2,6
platinum, native	(Pt,Fe) > 80 at. % Pt	Pd,Ir,Fe,Cu,Ni	x	xxx	2,6
platinum oxide	(Pt,O)?	Rh,Ir,Fe,Cu,Ni,Sb	xxx	-	1
Pt-Fe-Cu-Ni alloys**	(Pt,Fe,Cu,Ni)	Pd,Rh,Ir,Sb	-	x	1
rutheniridosmine	(Ru,Os,Ir)	Pt,Pd,Rh,Fe,Cu,Ni	xxx	x	5
sperryllite	PtAs ₂	Pd,Ni,Ru,Fe,Sb,S	xx	x	1,4,6
stumpflite	PtSb	Pd,Ru	-	x	4
tetraferroplatinum	PtFe	Pd,Rh,Ir,Cu,Ni,Sb	(xxx)	x	1
tolovkite***	IrSbS	Rh,As	-	x	3,6
tulameenite	Pt ₂ FeCu	Pd,Rh,Ir,Os,Ni,Sb	xx	xx	1,3
unnamed RhSbS	RhSbS	Pt,Ir,As	-	x	3,6

* only found as inclusions in one grain of gold; not derived from the Tulameen ultramafic complex.

** see text for nomenclature. *** Originally reported as unnamed IrSbS (6).

¹ Frequency: xxx = most common; xx = common; x = infrequent to rare; (xxx) = probably present in Pt-Fe-Cu-Ni alloys but not confirmed by XRD.

² References: 1. This study; 2. Cabri & Feather (1975); 3. Cabri *et al.* (1973); 4. St. Louis *et al.* (1986); 5. Harris & Cabri (1973); 6. Raicevic & Cabri (1976); 7. Cabri & Hey (1974).

rences. For example, the richer and more extensively exploited platinum deposits of the Urals contain sizeable concentrations of Pt-Fe alloys in bedrock, whose textures match the coarse intergrowths involving chromite and olivine in placer nuggets (*cf.* Duparc & Tikonowitch 1920).

CHEMISTRY OF CHROMITE AND SILICATE MINERALS

Analyses were conducted on selected grains of chromite, olivine and other minor silicate inclusions in platinum nuggets in order to compare their compositions with cumulate minerals in the Tulameen complex and to determine more precisely the source of the PGE mineralization. The analytical results are presented in Tables 10-12.

Chromite

The compositions of chromiferous spinel in placer nuggets and Tulameen chromitites are given in Table 10 and plotted in Figures 12 and 13. Spinel grains in the nuggets have high Cr (35.1-50.6 wt. % Cr₂O₃), highly variable Fe (11.9-28.2 wt. % Fe₂O₃) and rather low Al (6.0-8.7 wt. % Al₂O₃). The relatively high Fe³⁺ content of the spinel appears to be a general characteristic of Alaskan-type intrusions (Irvine 1967). The Holland nugget contains the most Cr-rich spinel; the Lincoln nugget exhibits appreciable intergrain zoning (35.1-39.2 wt. % Cr₂O₃). Spinel compositions within each M12410 nugget are

fairly uniform. Variations in Cr/(Cr + Al) on the whole are limited (0.79-0.83), and even more uniform within individual nuggets. No systematic differences in composition have been detected between spinel grains that seem to be completely encapsulated by Pt-Fe alloys and grains in areas of more massive chromite.

Most spinel grains in the nuggets fall within the compositional field of Tulameen chromitites, although the Lincoln nugget exhibits some overlap with spinel compositions encountered in dunite, and the Holland nugget contains the most Mg-rich, and ΣFe- and Fe³⁺-poor spinel (Figs. 12, 13). In general, chromite in the nuggets is quite distinct from the cumulus spinel in olivine- and hornblende-rich clinopyroxenites, which approaches the pure magnetite end-member in the latter rock-type (most clearly distinguished in Fig. 12). Cumulus spinel is comparatively rare in the more clinopyroxene-rich olivine clinopyroxenites, and typically absent in olivine-free clinopyroxenites. The absence of a spinel phase may be related to a reaction relationship between spinel and coexisting silicate melt at a point where Cr-bearing clinopyroxene becomes a dominant phase on the liquidus (Irvine 1967, Hill & Roeder 1974). The trend of spinel compositions in olivine clinopyroxenites away from the Cr-Al join in the cation plot (Fig. 13), and toward "ferritichromite" or Cr-bearing to Cr-free magnetite, reflects loss of Al (and Mg) and gain of Fe²⁺ and Fe³⁺ during low-temperature alteration (*e.g.*, Bliss & MacLean 1975, Evans &

TABLE 10. ELECTRON-MICROPROBE DATA ON CHROMITE IN CHROMITITES AND PLACER NUGGETS

Analysis:	Nuggets															Chromitites		
	LINCOLN						HOLLAND		MI2410					147	148	50		
	1	2	3	4	5	6	(n=8)* 7	(n=4)* 8	(n=2)* 9	(n=3)* 10	(n=2)* 11	(n=4)* 12	(n=3)* 13	(n=16)* 14	(n=12)* 15	(n=8)* 16		
SiO ₂	0.16	0.31	0.25	0.30	0.24	0.18	0.22	0.26	0.27	0.24	0.32	0.21	0.35	0.27	0.19	0.19		
TiO ₂	0.68	0.88	0.69	0.86	0.83	0.84	0.59	0.58	0.58	0.50	0.29	0.47	0.35	0.78	0.42	0.51		
Al ₂ O ₃	6.10	6.20	6.00	6.60	6.20	6.10	8.70	7.90	8.00	6.70	6.70	7.60	7.70	6.31	7.28	7.45		
Cr ₂ O ₃	39.20	35.40	35.50	37.80	36.00	35.10	50.60	48.30	48.80	48.70	49.20	47.50	47.70	37.03	43.65	49.01		
Fe ₂ O ₃ **	23.50	27.50	28.20	25.30	26.60	28.20	11.90	15.40	15.00	16.10	15.80	16.30	16.20	26.70	20.88	15.36		
FeO	22.60	20.20	19.50	21.80	22.00	22.70	14.90	15.90	16.10	17.50	17.50	17.00	17.10	20.71	18.40	17.20		
MnO	0.62	0.50	0.52	0.27	0.57	0.15	0.34	0.17	0.25	0.43	0.45	0.45	0.16	0.47	0.45	0.35		
MgO	6.60	8.50	8.70	7.90	7.20	7.10	12.20	11.60	11.60	10.30	10.20	10.60	10.80	7.96	9.57	10.49		
NiO	-	-	-	-	-	-	-	0.06	0.08	0.11	0.12	0.05	0.05	-	-	-		
ZnO	-	-	-	-	-	-	-	0.13	0.11	0.13	0.15	0.12	0.13	-	-	-		
Total	99.46	99.49	99.36	100.83	99.64	100.37	99.45	100.28	100.79	100.71	100.73	100.30	100.54	100.23	100.84	100.56		
Cations per 32 Oxygen atoms																		
Si	0.045	0.086	0.070	0.082	0.067	0.050	0.059	0.069	0.071	0.064	0.086	0.056	0.093	0.075	0.051	0.051		
Ti	0.144	0.183	0.144	0.177	0.174	0.175	0.118	0.112	0.115	0.101	0.058	0.094	0.070	0.162	0.085	0.103		
Al	2.011	2.018	1.955	2.125	2.033	1.991	2.710	2.466	2.484	2.113	2.114	2.394	2.413	2.042	2.301	2.338		
Cr	8.670	7.727	7.757	8.162	7.919	7.685	10.573	10.111	10.162	10.304	10.415	10.035	10.025	8.037	9.255	10.318		
Fe ³⁺	4.947	5.713	5.865	5.199	5.569	5.877	2.367	3.062	2.982	3.253	3.182	3.270	3.236	5.516	4.214	3.078		
Fe ²⁺	5.287	4.664	4.507	4.979	5.119	5.257	3.294	3.526	3.538	3.909	3.916	3.792	3.811	4.755	4.127	3.801		
Mn	0.147	0.117	0.122	0.063	0.135	0.036	0.077	0.038	0.056	0.097	0.102	0.102	0.036	0.110	0.103	0.079		
Mg	2.752	3.498	3.584	3.216	2.986	2.931	4.806	4.579	4.554	4.109	4.071	4.222	4.280	3.257	3.825	4.164		
Ni	-	-	-	-	-	-	-	0.013	0.017	0.024	0.026	0.011	0.011	0.000	0.000	0.000		
Zn	-	-	-	-	-	-	-	0.025	0.021	0.026	0.030	0.024	0.026	0.000	0.000	0.000		
Cr #	81.2	79.3	79.9	79.3	79.6	79.4	79.6	80.4	80.4	83.0	83.1	80.7	80.6	79.7	80.1	81.5		
Mg #	34.2	42.9	44.3	39.2	36.8	35.8	59.3	56.5	56.3	51.3	51.0	52.7	52.9	40.7	48.1	52.1		

* Average of n spot analyses. ** Calculated assuming ideal stoichiometry. Analyses 1-4, 8, 10, 12: chromite grains at rim of nugget. Cr # = 100Cr/(Cr+Al); Mg # = 100Mg/(Mg+Fe²⁺); Analyses 5-6, 9, 11, 13: chromite grains totally encapsulated by platinum alloy. Location of chromitite samples shown in Figure 2. - = not determined.

Frost 1975). As documented above, similar alteration is present at the margins of chromite grains in platinum nuggets. The compositional gap in the field for olivine clinopyroxenites (Figs. 12, 13) is probably an artifact of inadequate sampling, and most likely a continuum of compositions of variably altered, chromiferous spinel exists.

From the preceding data, it is clear that the abundance and composition of chromite in the nuggets point to a source of PGE-enriched placer material located within the dunite core of the Tulameen complex.

Olivine

Compositions of olivine grains in nuggets and ultramafic rocks of the Tulameen complex (Table 11) are plotted in Figure 14. The olivine in the nuggets has a composition extending from Fo_{93.2} to Fo_{95.2}, with little variation among, or within, the individual nuggets. These compositions are distinct from those in olivine clinopyroxenite (Fo₈₃-Fo₉₁) or dunite (Fo₈₈-Fo₉₁), and closely match olivine compositions in the Tulameen chromitites (Fo₉₂-Fo₉₅; Fig. 14). The limited number of dunite samples analyzed in this study is supplemented by data from Findlay (1963), who conducted more extensive sampling of the dunite core (Fig. 2). Although Findlay's data were obtained on mineral separates by an X-

ray-diffraction technique, his determinations are in good agreement with our microprobe analyses. The results clearly indicate that the dunite core as a whole is characterized by limited variation of olivine compositions.

The olivine compositions in these chromitites, however, are not primary. Numerous studies have pointed out the tendency for spinel and olivine to re-equilibrate under high-temperature, subsolidus conditions, such that Mg/(Mg+Fe²⁺) decreases in spinel and increases in olivine (e.g., Irvine 1965, Clark 1978). All other factors being equal, the degree of subsolidus exchange during slow cooling is dictated by mass-balance considerations, namely the relative modal abundance of chromite and olivine within the volume of effective equilibration. These effects can be quite pronounced on the scale of a single thin section. For example, analyses 7 and 8 in Table 11 represent averages of olivine compositions in dunite and chromitite at opposite ends of the same thin section. Significant differences exist between cumulate olivine (Fo₉₀) in dunite that contains approximately 1 vol. % spinel, and that trapped within part of a thin (3 cm) layer of chromitite containing approximately 5 vol. % olivine primocrysts (Fo₉₄). From these data, it is evident that the highly magnesian compositions characteristic of olivine in the platinum nuggets are an unmistakable and predictable signature of their chromitite heritage.

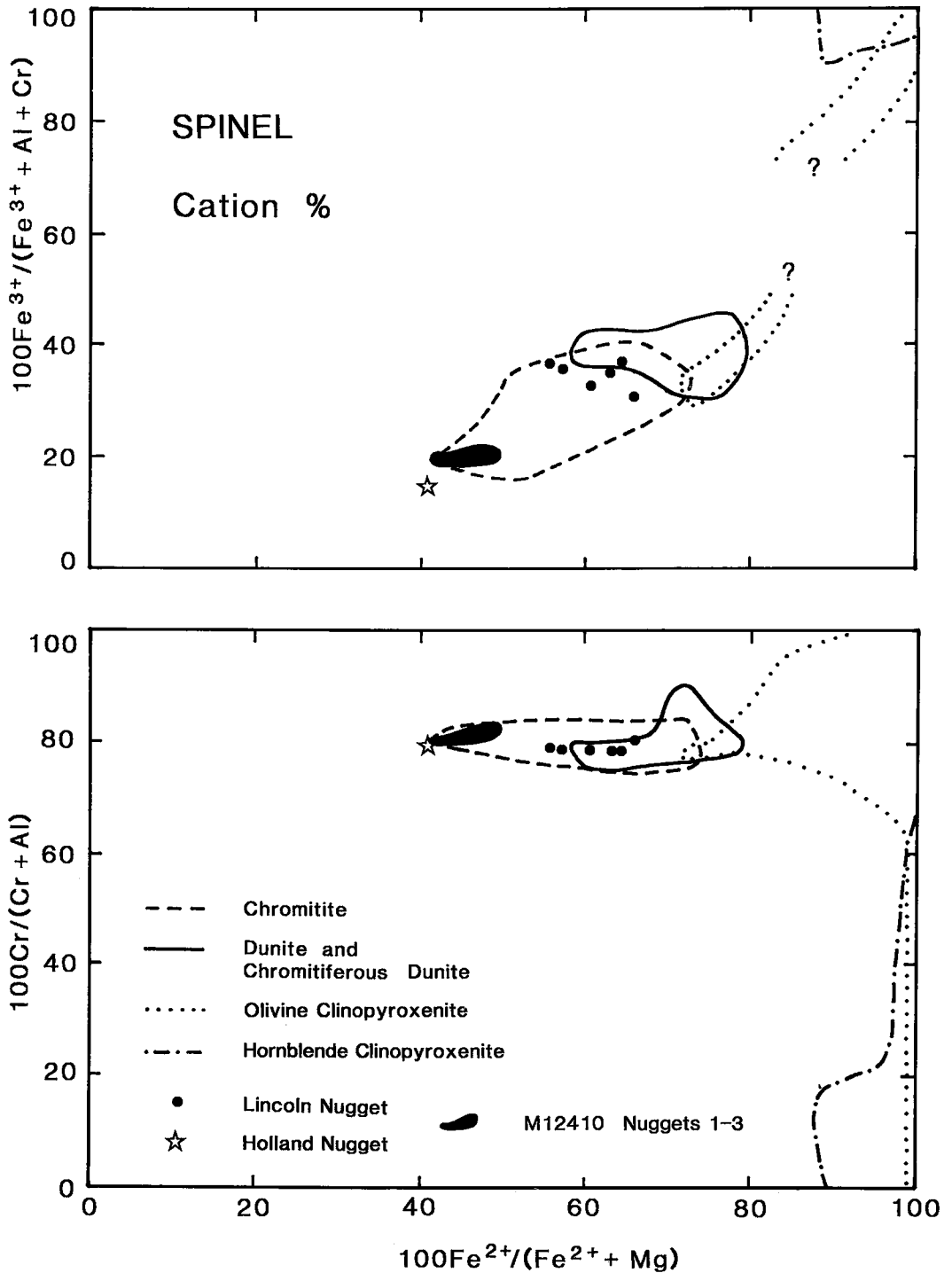


FIG. 12. Plots of $\text{Fe}^{2+}/(\text{Fe}^{2+} + \text{Mg})$ versus $\text{Cr}/(\text{Cr} + \text{Al})$ and $\text{Fe}^{3+}/(\text{Fe}^{3+} + \text{Al} + \text{Cr})$ for chromiferous spinel in placer nuggets (32 analyses) in comparison to spinel compositions (264 analyses) in major rock-types of the Tulameen complex.

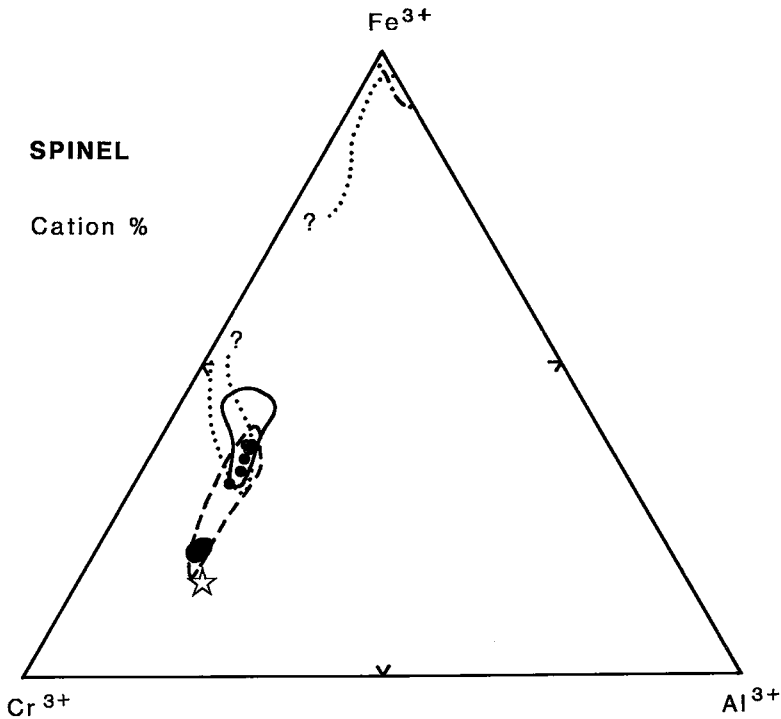


FIG. 13. Fe^{3+} -Cr-Al plot of spinel compositions in placer nuggets and major rock-types of the Tulameen complex. Same data and symbols as in Figure 12.

Silicate inclusions in nuggets

In addition to olivine, M12410 nuggets 1 and 3, and particularly nugget 1, contain a number of inclusions of primary and secondary silicates (Fig. 15). Representative compositions of the various minerals are given in Table 12 (*cf.* Fig. 10D), where the inclusion number identifies coexisting phases in specific inclusions. Silicates considered to be primary comprise clinopyroxene, hornblende, Fe-Mg mica (biotite-phlogopite) and plagioclase. Minerals indicative of secondary alteration principally include serpentine (compositions not given), chlorite and epidote, and trace amounts of quartz and sericite, and presumably represent the effects of subsequent regional metamorphism. Most inclusions are small (<200 μm across), incorporate more than a single mineral phase, and are hosted predominantly by platinum alloy (rarely chromite). They contain euhedral to anhedral crystals that rarely exceed 100 μm in length and average about 20–50 μm (Fig. 15).

Euhedral to subhedral *clinopyroxene* is a common inclusion mineral that occurs alone or is accompanied by plagioclase or phlogopite. Locally, it is intergrown with epidote and chlorite. In terms of the pyroxene quadrilateral (Morimoto 1989), clinopyroxene compositions extend along the diopside-

TABLE 11. ELECTRON-MICROPROBE DATA ON OLIVINE IN PLATINUM NUGGETS

	Nuggets						Tulameen Complex	
	Lincoln		Holland		M12410-3	Dunite	Chromite	
	1	2	3	4	5	6 (n=3)*	7 (n=6)*	8 (n=7)*
SiO_2	41.50	41.90	41.40	41.20	41.40	41.70	40.50	41.54
TiO_2	-	-	-	-	-	-	0.01	0.01
Al_2O_3	-	-	-	-	-	-	0.08	0.12
FeO	6.70	5.20	6.10	5.40	4.80	5.80	10.69	5.95
MnO	-	-	-	-	-	-	0.24	0.09
MgO	51.90	52.90	52.30	52.30	53.20	52.40	47.97	52.10
CaO	-	-	-	-	-	-	0.22	0.19
Total	100.10	100.00	99.80	98.90	99.40	99.90	99.71	100.00
	Cations per 4 Oxygen atoms							
Si	1.001	1.004	0.999	1.000	0.997	1.003	1.000	1.000
Ti	-	-	-	-	-	-	0.001	0.001
Al	-	-	-	-	-	-	0.003	0.004
Fe	0.136	0.105	0.124	0.110	0.097	0.117	0.221	0.120
Mn	-	-	-	-	-	-	0.006	0.002
Mg	1.865	1.889	1.881	1.892	1.910	1.879	1.766	1.869
Ca	-	-	-	-	-	-	0.006	0.005
XY	2.001	1.994	2.005	2.002	2.007	1.996	2.002	2.001
Z	1.001	1.004	0.999	1.000	0.997	1.003	1.000	1.000
Fo%	93.2	94.7	93.8	94.5	95.2	94.1	88.9	94.0

* Average of n spot analyses. Analyses of random grains at rim of nugget (1-3) and totally encapsulated within Pt-Fe alloy (4). Analysis 5: grain at rim of nugget. Analysis 6: olivine grain at rim of nugget in contact with tulameenite and platinum copper. Analyses 7 and 8 represent a microprobe traverse across a dunite-chromite contact in a thin section of sample GN87-159 (location shown in Figure 2). - not determined.

hedenbergite join from Mg-rich diopside [$100\text{Mg}/(\text{Mg} + \text{Fe}^{2+})$ or $\text{Mg}\# = 96.0$, inclusion 7] to Fe-rich diopside ($\text{Mg}\# = 58.6$, inclusion 2b), and are coincident with the trend for clinopyroxene in

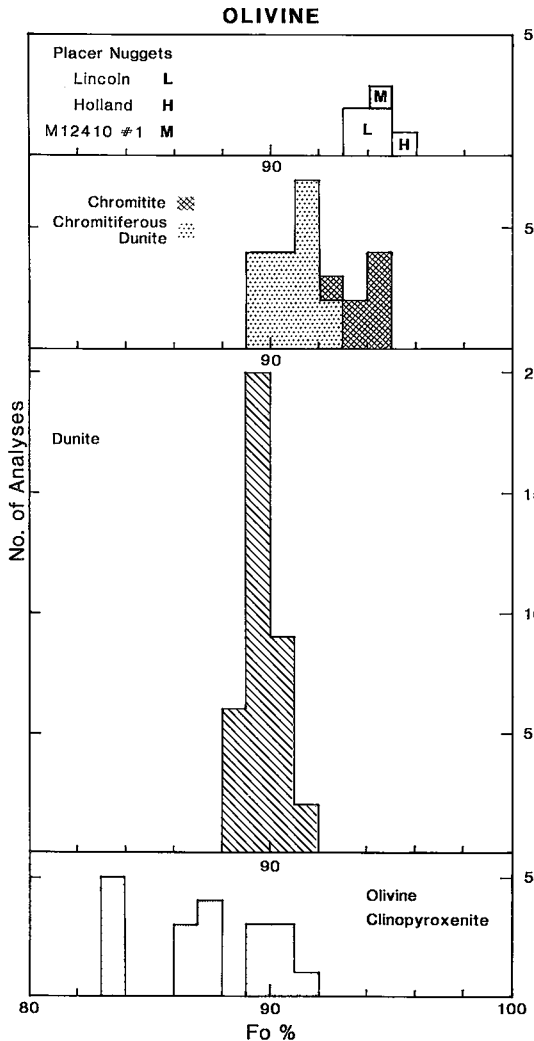


FIG. 14. Histogram showing the distribution of olivine compositions (% forsterite) in placer nuggets (8 spot analyses) and ultramafic rocks (80 analyses) of the Tulameen complex.

ultramafic rocks of the Tulameen complex (Fig. 16). The most iron-rich clinopyroxene compositions coexist with plagioclase (inclusions 2a-b).

The *plagioclase* (inclusions 2a-b, Table 12) is almost pure albite ($Ab_{96}-Ab_{98}$), and most probably reflects subsolidus re-equilibration of an originally more calcic plagioclase under conditions of greenschist-facies metamorphism; Ca may have been incorporated locally in epidote, which also is found within Pt-Fe alloy in the same nugget (inclusion 5, Table 12, Figs. 15C, 16). A magmatic origin for these plagioclase compositions is difficult to reconcile with

the extensive range of coexisting clinopyroxene compositions.

Single crystals of euhedral to subhedral *phlogopite* in chromite are more magnesian (Mg# 96.3-94.9) than cumulate phlogopite in olivine clinopyroxenite (Mg# 91.7; Table 12). This is also true for phlogopite coexisting with diopside (inclusion 7), which falls at the most "primitive" end of the clinopyroxene trend (Fig. 16).

Two 20- μ m crystals of *amphibole* and *biotite* in inclusion 1 are the most iron-rich silicates encountered. The biotite has relatively low Ti and a Mg# of 47. The coexisting calcic amphibole [$(Na + Ca)_B = 1.91$, $Na_B = 0.09$] is ferroan pargasitic hornblende (Leake 1978), with $(Na + K)_A = 0.92$, $Si = 6.55$ and a Mg# of 38. In comparison, cumulate amphibole and biotite primocrystals in hornblende clinopyroxenites of the Tulameen complex are significantly more magnesian (Table 12). According to Leake's classification, the hornblende in the clinopyroxenites is a relatively Mg-rich ferroan pargasite having a low Si (6.18) and a Mg# of 65.

Chlorite and *epidote* locally replace phlogopite and plagioclase, respectively. However, some chlorite may have been formed by reaction of serpentine and chromite to produce chlorite and "ferritchromite" (P. L. Roeder, pers. comm. 1990). The chlorite is Mg-rich clinocllore, with little variation in Mg#. Both phases contain significant quantities of Cr, reaching 3.5 wt. % Cr_2O_3 in chlorite and 4.1 wt. % in epidote. Recently, Pan & Fleet (1989) reported up to 3.5 and 11.8 wt. % Cr_2O_3 in chlorite and epidote, respectively, from metasomatically altered komatiites and komatiitic basalts in Ontario; Stockman & Hlava (1984) identified chromian chlorite (4.2 wt. % Cr_2O_3) in PGE-bearing Alpine-type chromitites from southwestern Oregon. Thus, it appears that in the absence of primary silicates, Cr-bearing secondary minerals in placer nuggets may provide important clues as to the ultramafic provenance of the PGE mineralization.

DISCUSSION

Origin of PGE-rich nuggets

If the PGE-rich placer nuggets were derived from the chromitite horizons that were sampled in the core of the Tulameen complex, we would expect to see similar distributions of PGM in nuggets and chromitites. As pointed out above, and summarized in Table 9 and Figure 6, certain differences exist in the size, composition and relative abundance of PGM in placer and bedrock material. Discrepancies in the grain size of platinum alloys between nuggets and chromitites (mm-scale versus μ m-scale, respectively) can be rationalized as an artifact of sampling bias. That the nuggets did in fact come from an igneous

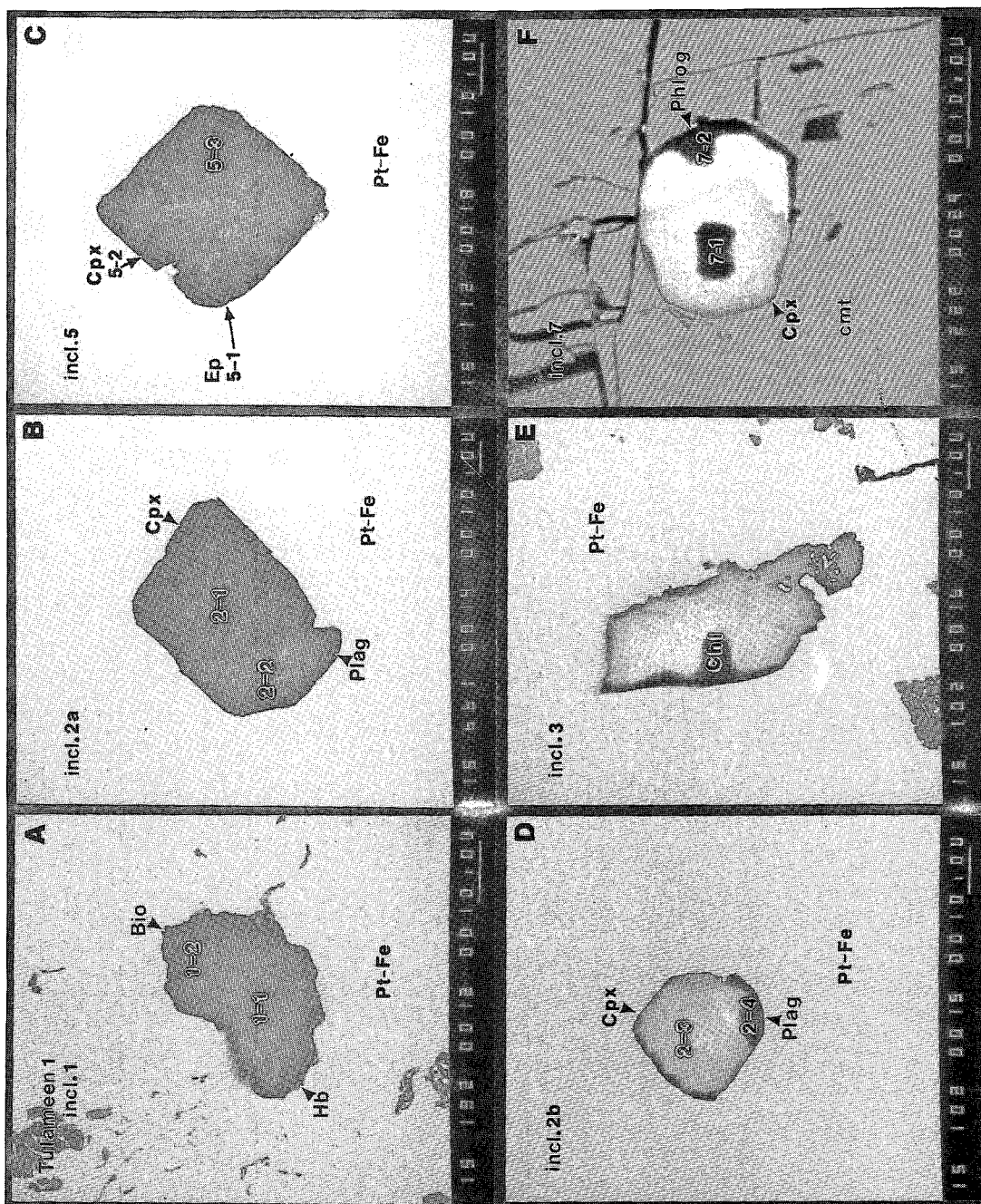


FIG. 15. SEM photomicrographs of silicate inclusions hosted by platinum alloy (Pt-Fe) and chromite (cmt) in nugget M12410-1 (cf. Table 12 and Fig. 10D). A. Coexisting Fe-rich biotite (Bio) and ferroan hornblende (Hb). B. Coexisting euhedral crystals of Fe-rich clinopyroxene (Cpx) and plagioclase (Plag). C. Subhedral clinopyroxene (Cpx) intergrown with epidote (Ep) and sericite (5-3) possibly pseudomorphous after plagioclase. D. Coexisting faceted crystals of Fe-rich clinopyroxene (Cpx) and plagioclase (Plag). E. Anhedral chlorite (Chl), possibly pseudomorphous after phlogopite, and minor serpentine (lower right, not readily visible). F. Partly faceted diopside (Cpx) and Mg-rich phlogopite (Phlog). Bar scale in μm .

TABLE 12. ELECTRON-MICROPROBE DATA ON MINOR SILICATE INCLUSIONS IN PLATINUM NUGGETS

Host: Inclusion No.;	Nuggets												Tulameen Complex									
	M12410-1										M12410-3		163	179	88	88						
Mineral:	PtFe 1	PtFe 1	PtFe 2a	PtFe 2a	PtFe 2b	PtFe 2b	PtFe 5	PtFe 5	Cmt 7	Cmt 7	Cmt (n=6)*	Cmt 5	Phlog	Phlog	Phlog	Phlog	Phlog	Phlog	Hb	Hb	Bi	
SiO ₂	42.10	35.20	54.00	69.00	53.10	68.50	38.50	53.80	54.60	39.90	30.70	38.60	54.42	38.79	52.05	41.40	37.30	54.42	38.79	52.05	41.40	37.30
TiO ₂	0.52	1.30	0.00	0.06	0.09	0.00	0.18	0.09	0.06	0.22	0.06	0.30	0.14	0.80	0.27	1.88	2.97	0.14	0.80	0.27	1.88	2.97
Al ₂ O ₃	10.60	13.30	0.59	19.50	0.15	19.90	25.10	1.00	0.73	13.80	14.70	15.00	0.75	14.91	2.15	12.40	15.80	0.75	14.91	2.15	12.40	15.80
Cr ₂ O ₃	0.16	0.00	0.00	0.00	0.00	0.10	0.09	0.13	1.30	2.00	2.87	2.20	0.44	0.39	0.00	0.00	0.00	0.44	0.39	0.00	0.00	0.00
FeO	21.30	22.30	7.60	0.21	12.70	0.25	10.00	6.60	1.30	2.50	1.93	1.90	2.11	4.29	7.54	12.80	13.59	2.11	4.29	7.54	12.80	13.59
MnO	0.29	0.06	0.18	0.06	0.18	0.00	0.11	0.17	0.17	0.00	0.09	0.14	0.00	0.00	0.22	0.12	0.22	0.00	0.00	0.22	0.12	0.22
MgO	7.40	10.90	12.90	0.15	10.10	0.16	0.00	13.40	17.70	26.30	35.92	27.70	17.27	26.67	14.25	13.36	16.93	17.27	26.67	14.25	13.36	16.93
CaO	10.90	0.25	24.10	0.28	25.00	0.42	24.20	23.40	26.30	1.10	0.02	0.00	25.27	0.10	23.69	12.26	0.00	25.27	0.10	23.69	12.26	0.00
Na ₂ O	2.70	0.00	0.85	10.20	0.00	9.80	0.00	1.40	0.19	0.29	0.06	0.00	0.10	0.00	0.25	1.67	0.08	0.10	0.00	0.25	1.67	0.08
K ₂ O	1.00	7.90	0.00	0.30	0.00	0.00	0.00	0.00	0.00	7.20*	0.02	8.40	0.00	9.16	0.04	1.69	9.02	0.00	9.16	0.04	1.69	9.02
Total	96.97	91.21	100.22	99.76	101.32	99.13	98.18	99.99	102.35	93.31	86.37	94.24	100.50	95.11	100.46	97.58	95.91	100.50	95.11	100.46	97.58	95.91
Cations per number of Oxygen atoms																						
No. of Oxygens	23	22	6	8	6	8	25	6	6	22	28	22	6	22	6	23	22	6	22	6	23	22
Si	6.546	5.690	2.008	3.010	2.002	3.002	6.165	1.997	1.949	5.692	5.880	5.475	1.973	5.510	1.932	6.180	5.485	1.973	5.510	1.932	6.180	5.485
Ti	0.061	0.159	0.000	0.002	0.003	0.000	0.022	0.003	0.002	0.024	0.009	0.032	0.004	0.086	0.008	0.212	0.329	0.004	0.086	0.008	0.212	0.329
Al	1.943	2.534	0.026	1.003	0.007	1.028	4.737	0.044	0.031	2.320	3.319	2.508	0.033	2.496	0.095	2.182	2.739	0.033	2.496	0.095	2.182	2.739
Cr	0.020	0.000	0.000	0.000	0.000	0.000	0.012	0.004	0.037	0.226	0.435	0.247	0.013	0.044	0.000	0.000	0.000	0.013	0.044	0.000	0.000	0.000
Fe	2.770	3.015	0.237	0.008	0.401	0.010	1.340	0.205	0.039	0.299	0.310	0.226	0.064	0.510	0.234	1.598	1.672	0.064	0.510	0.234	1.598	1.672
Mn	0.039	0.009	0.006	0.003	0.006	0.000	0.015	0.006	0.006	0.000	0.015	0.017	0.000	0.000	0.007	0.016	0.028	0.000	0.000	0.007	0.016	0.028
Mg	1.715	2.626	0.715	0.010	0.568	0.011	0.000	0.742	0.942	5.592	10.254	5.856	0.933	5.647	0.789	2.973	3.711	0.933	5.647	0.789	2.973	3.711
Ca	1.816	0.044	0.950	0.014	1.010	0.020	4.152	0.931	1.006	0.169	0.005	0.000	0.982	0.016	0.942	1.961	0.000	0.982	0.016	0.942	1.961	0.000
Na	0.814	0.000	0.062	0.863	0.000	0.833	0.000	0.101	0.014	0.081	0.023	0.000	0.008	0.000	0.018	0.484	0.023	0.008	0.000	0.018	0.484	0.023
K	0.199	1.629	0.000	0.017	0.000	0.000	0.000	0.000	0.000	1.311	0.005	1.520	0.000	0.000	1.660	0.002	1.692	0.000	0.000	1.660	0.002	1.692
X	2.83	1.63	2.01	0.92	1.99	0.87	4.19	2.03	1.98	1.39	12.25	1.52	2.03	1.66	2.03	2.77	1.72	2.03	1.66	2.03	2.77	1.72
Y	5.09	6.08					6.09			6.32		6.38		6.31		5.16	5.96		6.31		5.16	5.96
Z	8.00	8.00	2.01	4.01	2.00	4.04	6.16	2.00	2.05	8.00	8.00	7.98	2.00	8.00	2.00	8.00	8.00	2.00	8.00	2.00	8.00	8.00
Ca (An)	28.8		50.2	(1.6)	51.0	(2.3)		49.6	50.6				49.6		47.9	30.0		49.6		47.9	30.0	
Mg (Ab)	27.2		37.4	(96.5)	28.7	(97.7)		39.5	47.4				47.2		40.1	45.5		47.2		40.1	45.5	
Fe (Or)	44.0		12.4	(1.9)	20.3	(0.0)		10.1	2.0				3.2		12.0	24.5		3.2		12.0	24.5	
Mg #	38.2	46.6	75.1		58.6			78.4	96.0	94.9	97.1	96.3	93.6	91.7	77.1	65.0	68.9	93.6	91.7	77.1	65.0	68.9

* Average of 6 random grain analyses. Mg # = 100 Mg/(Mg + Fe²⁺). † low K₂O probably due to loss of K in electron beam.

Hb - hornblende; Bi - biotite; Cpx - clinopyroxene; Plag - plagioclase; Ep - epidote; Phlog - phlogopite; Ch - chlorite; Cmt - chromite; PtFe - platinum-iron alloy; Ol Cpxite - olivine clinopyroxenite; Hb Cpxite - hornblende clinopyroxenite.

source is implied by the common incorporation of euhedral to subhedral crystals of cumulus chromite and minor olivine that are partly to completely enclosed by platinum alloy.

The compositions of chromite and olivine provide a more definitive argument for the origin of the *PGE* mineralization in the placers. The chromite found in nuggets exhibits significant variation in Mg# from nugget to nugget, but little difference in Cr/(Cr + Al). Within individual nuggets, however, compositions are more uniform. The majority of the grains analyzed plot in the field of Tulameen chromites, although some overlap exists with spinel compositions in dunite. From chromite chemistry alone, it might be inferred that there is probably more than one host rock (dunite and chromitite) with anomalous abundances of *PGE*.

In this respect, olivine compositions are particularly informative. The olivine in nuggets is much more magnesian (Fo₉₃-Fo₉₅) than its counterpart in Tulameen dunite (Fo₈₈-Fo₉₁), but identical in composition to minor amounts of olivine trapped in cumulus chromitites. Thanks largely to earlier work by Findlay (1963), the distribution of olivine compositions determined throughout the dunite core of the complex is unusually dense, which allows the construction of olivine isopleths (Fig. 2). These data show that the anomalously magnesian compositions of olivine are clearly unique to the chromitite

environment. Furthermore, it has been shown in numerous studies that if chromite and olivine are allowed to re-equilibrate upon cooling, the Mg# of olivine will increase in proportion to the modal abundance of chromite in the host, and an opposite and corresponding change occurs in coexisting chromite. Thus, the extremely magnesian compositions encountered in nugget olivine are a predictable consequence of cooling within a chromitite layer. Since it is not possible to rationalize the differences in *PGM*, placer nuggets must have been derived from chromitites that have not been sampled. The chromitite source of the *PGE* mineralization is no longer in question.

Significance of the inclusions of primary silicates

Besides chromite and olivine, primary inclusions in platinum alloys are represented by Mg-Fe mica (phlogopite-biotite), hornblende, clinopyroxene and plagioclase. Regional metamorphism was not sufficiently intense to obliterate the primary compositions of ferromagnesian silicates in the Tulameen complex, although plagioclase in the gabbroic rocks and in hornblende-rich pegmatites is commonly saussuritized (Findlay 1963, Nixon & Rublee 1988). It seems likely, therefore, that the ferromagnesian silicates reveal certain peculiarities in the crystallization history of *PGE*-bearing chromitites, particularly nug-

get M12410-1, which contains the most extensive suite of inclusions.

Whereas chromite and olivine are cumulus grains that have compositions compatible with early crystallization and re-equilibration within the chromitite environment, the inclusion minerals are more than an order of magnitude smaller ($< 100 \mu\text{m}$) and compositionally diverse. Mg-rich, Cr-bearing phlogopite (Table 12) possibly has re-equilibrated with chromite during subsolidus cooling in exactly the same manner as olivine (P. L. Roeder, pers. comm. 1990), or may have crystallized from the final few percent of trapped intercumulus melt (Roeder & Campbell 1985). Considering the presence of Fe-rich biotite in the same nugget, and coexisting ferroan pargasitic hornblende (inclusion 1, Table 12), the former explanation seems unlikely. The extensive range of clinopyroxene compositions also is noteworthy (Fig. 16). The Fe-rich clinopyroxene coexists with plagioclase (altered); such Fe-rich compositions extend beyond the range of clinopyroxene compositions found in ultramafic rocks of the Tulameen complex. Such clinopyroxene, and probably the hydrous Fe-rich silicates, evidently crystallized from melts of gabbroic or dioritic composition.

The observations noted above may be rationalized with the textures and compositions of chromite and olivine if the silicate inclusions represent the products of fractionation of primitive melt trapped in Pt-Fe alloy at the time of chromitite formation. From the olivine-chromite re-equilibration, we know that cooling was slow enough to permit high-temperature solid-state diffusion, and these conditions would certainly favor continued crystallization of any pockets of melt. The trapped liquid can be perceived as a microcosm of large-scale crystal-melt fractionation processes operating in the Tulameen magma chambers. According to this hypothesis, the most Fe-rich clinopyroxene compositions in the inclusions would represent the products of presumably closed-system evolution of felsic residual liquids, and may predict pyroxene trends in the syenogabbros and syenodiorites of the Tulameen complex, should such a model apply. Compositional data for pyroxene in the latter rocks are currently lacking.

Perhaps the most surprising aspect of the inclusion data is that cooling was sufficiently rapid to promote fractional crystallization of the trapped melt, although the implied thermal regime applies only to a single platinum nugget (M12410-1). Intriguingly, the platinum alloys serve as an almost ideal inert container for Nature's crystallization experiments, analogous to those regularly conducted in modern petrological laboratories, except that we are left to derive the experimental conditions of the charge! However, the problems are compounded, because there has been more than one experiment: the products of metamorphism (and any deuteric

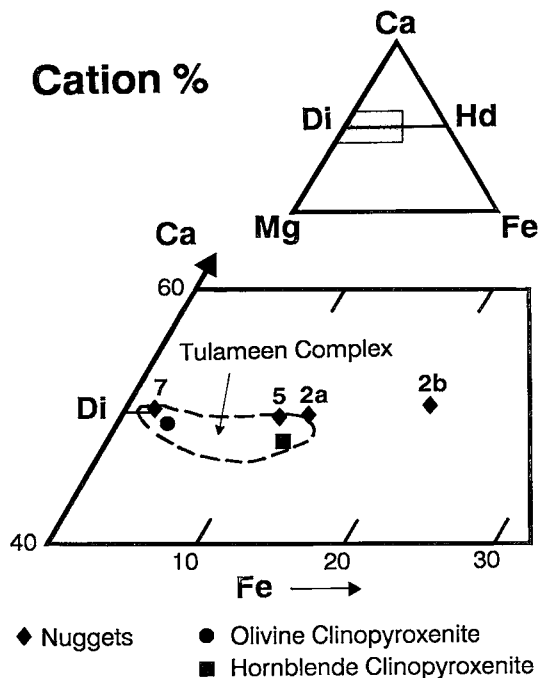


Fig. 16. Ca-Mg-Fe plot showing clinopyroxene compositions found in platinum nuggets and ultramafic rocks of the Tulameen complex (G. T. Nixon, unpubl. data). Numbers refer to inclusion no. (Table 12). Representative compositions of pyroxene in olivine and hornblende clinopyroxenites are given in Table 12.

changes that may have taken place) have formed subsequently both in the alloy (e.g., magnetite) and from primary silicates (e.g., chlorite and epidote).

Paragenesis of the PGM

The mode of occurrence and textural relationships of the PGM and associated base-metal minerals described earlier have been used to establish a tentative scheme of mineral paragenesis (Table 13). The PGM are subdivided into two groups: predominantly platinum-bearing alloys that are considered to have segregated from high-temperature silicate melts, and other PGM and base-metal minerals that are considered to have formed during later metamorphism and serpentinization.

The euhedral nature of platinum alloys locked in chromite (e.g., Figs. 4A, B, 5), the large grains of intercumulate alloys in nuggets that enclose cumulate olivine and chromite (e.g., Figs. 9A, 10), and their demonstrated association with concentrations of chromite in the dunite core of the Tulameen complex, leave little doubt that these early PGM represent the products of high-temperature crystallization of primitive mantle-derived magmas.

TABLE 13. PARAGENESIS OF PGM AND ASSOCIATED MINERALS

Early PGM (High-T, magmatic)	Late PGM, Base and Precious Metals (Low-T, hydrothermal)
Cooperite	Cu oxide
Erllichmanite	Genkinite
Ir-Pt alloys	Geversite
Laurite	Ni sulfides
Pt-Fe-Cu-Ni alloys	Ni antimonides
Ru-Os-Ir alloys	Ni arsenides
	Native copper
	Native silver
	Ni oxide
	Platinian copper
	Pt oxide
	Rh-Ir(AsS)
	RhSbS
	Sperrylite
	Tolovkite
	Tulameenite

The coprecipitation of Pt-Fe alloys and chromite in Alaskan-type intrusions has recently been addressed by Amossé *et al.* (1990), who investigated the solubility of Pt and Ir in a basaltic melt. Based on thermodynamic considerations and experimental data, they showed that an increase in $f(\text{O}_2)$ decreases the solubility of Pt and Ir in the melt, and argued that Pt-Fe alloys with 10% Fe may precipitate in Pt-saturated melts at typical basaltic liquidus temperatures and oxygen fugacities of approximately 10^{-6} bar, conditions that enhance the precipitation of chromite (Hill & Roeder 1974). Since Pt is more soluble than Ir under a wide range of $f(\text{O}_2)$ and $f(\text{S}_2)$ conditions, the precipitation of Pt-Fe alloys in nature ought to be accompanied by Ir-rich phases. The predicted consequences of magmatic crystallization are observed in the Tulameen complex, in which the precipitation of chromite and Pt-Fe-Cu-Ni alloys (containing significant amounts of Ir in solid solution; Tables 2A, B) is accompanied by rare iridium, osmiridium, and platiniridium (Table 9). The preponderance of Pt-rich as opposed to Ir-rich phases in the chromitites of the Tulameen complex presumably reflects the high overall Pt/Ir ratio of parental magmas.

By analogy with relationships in the system Pt-Fe (Heald 1967), the considerable range of compositions of platinum alloy along the Pt-Fe join in Figure 6 is as expected if complete solid-solution exists at liquidus temperatures typical of basaltic systems (1300–1200°C). However, there is evidence that some of the early Pt-Fe-Cu-Ni alloy compositions may have undergone high-temperature subsolidus modification during cooling. The tie lines for two

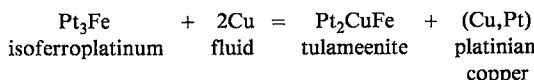
coexisting pairs of alloys from the same chromite layer (Table 2A), including at least one zoned, euhedral crystal (Fig. 5), straddle a compositional gap separating “tetraferroplatinum” [Pt(Fe,Ni,Cu)] and “isoferroplatinum” [Pt_{2.5}(Fe,Ni,Cu)_{1.5}] (Fig. 6). These relationships suggest the presence of a miscibility gap in the system Pt-Fe-Ni-Cu, analogous to that implied to exist at low temperatures between pure Pt₃Fe and PtFe (Cabri & Feather 1975). However, intimate, eutectic-like intergrowths of these alloys, such as those described by Johan *et al.* (1989) for nearly pure Pt-Fe phases, have not been observed.

Even though the faceted crystals shown in Figure 5 that are contained in chromite appear to have grown from a melt, several internal features seem somewhat unusual for a growth phenomenon: the extremely variable thickness of the “isoferroplatinum” rim, its sharp contact with “tetraferroplatinum” in the core, and the highly irregular contact between these phases. We speculate that the zoning in this crystal may represent a reaction texture whose origin is intimately linked to its chromite host. For example, Naldrett & Lehmann (1987) pointed out that where sulfide and chromite coexist, structural vacancies in chromite can be expected to take up Fe on cooling and thus promote desulfurization reactions whereby the proportion of base-metal sulfides decreases, and elements like Cu, Ni and PGE are concentrated in the remaining sulfides. A similar mechanism may also explain the zoned inclusions of platinum alloys in chromite. Loss of Fe from Pt-Fe alloy to fill vacancies in chromite could produce “isoferroplatinum” on cooling within a miscibility gap in the platinum alloy system. If this suggestion is viable, Ni and Cu must be removed along with Fe (*cf.* Fig. 6B, C), and “tetraferroplatinum” may represent a relict, high-temperature composition. This explanation is only applied to the formation of “isoferroplatinum” in this particular chromitite.

Textural evidence suggests that the late PGM (Table 13) resulted from *in situ* metasomatic replacement of platinum alloy primocrysts (*e.g.*, Figs. 3, 4C, D, 7B, 11D) and limited localized fracture-filling within the chromite host (*e.g.*, Figs. 3B, 7A, B). Thus, the mobility of PGE during hydrothermal alteration appears to be rather limited.

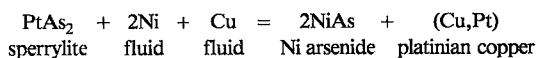
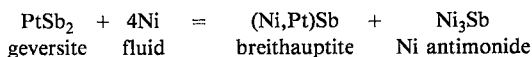
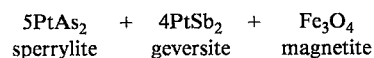
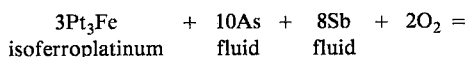
The only Pt-Fe-Cu-Ni alloy that is clearly secondary is tulameenite, which is intimately associated with platinian copper in both nugget and lode occurrences. Platinian copper is intergrown with a variety of products of late-stage crystallization that are enclosed in serpentine, including secondary magnetite that is presumably derived from the breakdown of olivine (Fig. 8C). In one chromitite, tulameenite forms an intimate intergrowth with isoferroplatinum(?) and appears to partly replace the euhedral Pt-Fe-Ni-Cu alloy grain (Figs. 4C, D). An equation

may be written that describes this reaction in the presence of an aqueous fluid:



The presence of native copper in carbonate-serpentine veinlets that cut chromitites (Fig. 8D) indicates a relatively high activity of Cu and low $f(\text{S}_2)$ in the fluid phase, and suggests that reactions of this type are indeed pertinent to the genesis of certain of the copper-rich *PGM*.

Textural relationships among platinum alloys, sperrylite and geversite seem somewhat ambiguous. The latter two minerals are found as fracture fillings in chromite (Figs. 3B, 7A, B) and as subhedral grains located on fractures (Figs. 3D, 7B). In addition, geversite forms complex intergrowths with Ni antimonides and platinian copper (Figs. 7C, 8A). The common association of geversite with base-metal antimonides in serpentine suggests a low-temperature hydrothermal origin and is also compatible with the presence of geversite along fractures in chromite (Fig. 7A). Where certain fractures exposed primary platinum alloys to the action of hydrothermal fluids, some grains were completely transformed to Pt antimonides and arsenides (Figs. 3D, 7B). Breithauptite and platinian copper locally have formed later than geversite (Figs. 7C, D, 8A), and these minerals are commonly intergrown with Ni arsenides and antimonides (Fig. 8B). Equations of the type:



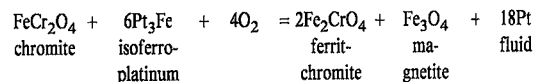
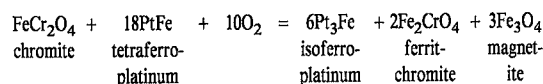
can potentially explain these observations. Textural evidence for equilibrium between geversite and sperrylite is lacking.

Small quantities of Pt detected in Ni antimonides appear to decrease in proportion to increasing Ni/Sb in the antimonides (Table 6). The nickel in antimonides and arsenides is readily available *via* serpentinization of olivine in host dunite. The copper and antimony may well have been derived from outside the Tulameen complex by leaching of host rocks that make up the Nicola Group.

Rh-Ir sulfarsenides partly replace primary platinum

alloys (Figs. 3B, C) and probably formed more or less contemporaneously with Pt arsenides and antimonides. The formation of rare Pt oxide (*e.g.*, Figs. 7C, D) shows clear evidence of alteration under conditions of locally high $f(\text{O}_2)$.

Intergrowths of magnetite in platinum alloy also appear to have formed in response to conditions of elevated oxygen fugacity, and are linked with serpentinization and hydrothermal alteration of chromite. The abundance of fine magnetite intergrowths in platinum alloy adjacent to chromite (Figs. 9B, 10D) strongly suggests a low-temperature reaction relationship. Relevant equations may be represented by:



Platinum may be immobile, and loss of Fe from tetraferroplatinum may form magnetite and "ferrit-chromite" in an isoferroplatinum reaction product. Alternatively, platinum may enter the fluid phase and take part in localized reactions involving antimonides and arsenides, as described earlier. Another possibility is that part of the platinum enters the magnetite structure, as postulated by Cabri *et al.* (1981). The fine-grained nature of secondary magnetite in the Tulameen nuggets precluded confirmation of the latter hypothesis.

Sulfides

Sulfide minerals identified in lode and placer occurrences include extremely rare *PGM* (erlichmanite and laurite) and base-metal sulfides (pyrite, millerite or heazlewoodite, pentlandite, violarite, bravoite, rare chalcopyrite, and an undetermined Ni-Co-Fe sulfide). The presence of pyrrhotite has not been confirmed. Erlichmanite and laurite are associated with platinum alloys and are considered to have a high-temperature origin. Laurite, in particular, has been observed with a faceted morphology. In chromitites, the sulfides are invariably found in the interstices among chromite grains associated with serpentine, magnetite, and secondary *PGM*; no sulfides have been observed to coexist with primary Pt-Fe-Cu-Ni alloys enclosed in chromite. In one nugget, however, pentlandite and chalcopyrite have been identified in Pt-Fe alloy, but not without other secondary oxides (magnetite) and *PGM* (*e.g.*, irarsite; *cf.* Raicevic & Cabri 1976).

St. Louis *et al.* (1986) made similar observations but proposed that some sulfides, in particular pentlandite, had a relatively high-temperature, magmatic

origin. However, their illustration of this type of paragenesis (St. Louis *et al.* 1986, Fig. 2B) involves an intergrowth of serpentine, magnetite, pentlandite, sperrylite and irarsite within a fractured area in chromite. Although the possibility of trace amounts of magmatic base-metal sulfides, albeit remobilized, cannot be categorically ruled out, this mineral assemblage is quite consistent with a low-temperature, hydrothermal paragenesis, as implied earlier.

PGE mineralization in Alaskan-type complexes

In Alaskan-type complexes in general, the chromitite-*PGE* association appears to be the most widespread type of lode mineralization, though not the sole economic target (*cf.* Cox & Singer 1986, Nixon & Hammack 1990). In fact, *PGE*-enriched chromitites are even more important in other geological environments, such as stratiform mafic intrusions (*e.g.*, Bushveld, South Africa; Stillwater, Montana; and Bird River sill, Manitoba), and also have potential in the Alpine-type or ophiolitic (podiform) settings (*e.g.*, Shetland ophiolite, Prichard *et al.* 1986). The podiform chromitites are usually impoverished in Pt and Pd relative to Ru, Os, Ir (*e.g.*, Legendre & Augé 1986), as are some stratiform chromitites (*e.g.*, Bird River and most Stillwater chromitites, Cabri & Laflamme 1988, Talkington & Watkinson 1986). However, certain stratiform chromitites (*e.g.*, those in the Middle and Upper Groups of the Bushveld and the A chromitite of the Stillwater complex) exhibit anomalous enrichment of Pt and Pd, although not as extreme as that encountered in the *PGE*-rich, sulfide-bearing reefs such as the Merensky (Bushveld) and J-M (Stillwater), which are characterized by extremely high (Pt + Pd)/(Ru + Os + Ir) ratios (Naldrett *et al.* 1987, Lee & Parry 1988).

In order to explain differences in the distribution and abundances of *PGE* between chromitites from layered intrusive and ophiolitic complexes, Naldrett & Von Gruenewaldt (1989) proposed that the concentration of Pt and Pd in stratiform chromitites, and high (Pt + Pd)/(Ru + Os + Ir) ratios, reflect the former presence of base-metal sulfide in the chromitites. The original process of concentration of the *PGE* is perceived to be that of collection by a Fe-Cu-Ni-rich sulfide liquid. Subsequent crystallization of non-sulfide *PGM* is accomplished during cooling at high temperatures, and the desulfurization reactions are driven by subsolidus uptake of sulfide-hosted Fe by chromite (Naldrett & Lehmann 1987). They concluded that such a process could account for high concentrations of *PGE* in chromitites with little or no visible sulfide, and that high (Pt + Pd)/(Ru + Os + Ir) ratios indicate appreciable content of original sulfide.

The textural and mineralogical data presented

above for the Tulameen complex do not support such a mechanism for chromitite-associated *PGE* mineralization in Alaskan-type intrusions. The *PGE* are primarily contained in Pt-Fe and Pt-Ir alloys, and, just as in the majority of Alaskan-type complexes, are not associated with primary magmatic base-metal sulfides (Cabri 1981). We note that the high (Pt + Pd)/(Ru + Os + Ir) ratios of *PGE*-enriched chromitites in the Tulameen and other Alaskan-type complexes are typically accompanied by high Pt/Pd (*e.g.*, Nixon & Hammack 1990). The latter feature appears inconsistent with collection by base-metal sulfides, which are known to concentrate both Pt and Pd (*e.g.*, Makovicky *et al.* 1986, Talkington & Watkinson 1986, Naldrett 1989). In the case of the Tulameen and many other Alaskan-type intrusions, the concentration of *PGE* in chromitites is best explained by the accumulation of platinum-rich alloys that segregated directly from the melt at an early stage in the evolution of the complex.

CONCLUSIONS

The study described above has been directed toward a better understanding of the nature and origin of disseminated *PGE* mineralization in the Tulameen complex, a mafic-ultramafic intrusion of the Alaskan type, and spatially associated placers. The anomalously high concentrations of *PGE* in Tulameen chromitites and placers is explained by the presence of discrete primary and secondary *PGM*. Key features of the primary *PGM*, predominantly represented by Pt-Fe alloys with minor but significant abundances of Cu and Ni, are their idiomorphic habit in chromitites and coarsely crystalline texture in nuggets, in which platinum alloys enclose cumulus chromite and olivine. Secondary *PGM*, chiefly Pt arsenides and antimonides, Rh-Ir sulfarsenides, tulameenite and platinum copper developed locally in *PGE*-enriched host rocks by metasomatic replacement and limited remobilization of primary platinum alloys. The latter *PGM* were produced during subsequent serpentinization and regional metamorphism, and are associated with secondary low-temperature base-metal sulfides, arsenides and oxides.

Although differences exist in the nature and frequency of the *PGM* between bedrock and placer occurrences, coexisting gangue minerals confirm their derivation from a common source. In particular, the compositions of chromite and olivine in placer nuggets match those observed in chromitites in the dunite core of the Tulameen complex. Olivine is especially diagnostic because of its well-known tendency to re-equilibrate with chromite on cooling to produce anomalously magnesian compositions. Intriguingly, one nugget contains inclusions of other primary silicates with a wide range of compositions

that crystallized from silicate melts largely trapped in platinum alloys at the time of chromitite formation. These products of crystallization appear to mimic the liquid line of descent recorded by cumulate minerals in the ultramafic rocks of the Tulameen complex, and may reproduce the compositions of iron-rich clinopyroxene in gabbroic magmas that would evolve during comagmatic, closed-system fractional crystallization.

Finally, we stress that the high-temperature PGM segregated directly from a silicate melt and were not generated by exsolution from chromite or magmatic sulfides. The common association of Pt-Fe alloys and chromitites in Alaskan-type intrusions suggests that whatever mechanism triggers chromite precipitation in excess of normal cotectic proportions [e.g., increase in $f(\text{O}_2)$] also enhances or initiates the precipitation of Pt-Fe alloys from primitive parental magmas of the Alaskan-type association.

ACKNOWLEDGEMENTS

This project was funded by the Canada - British Columbia Mineral Development Agreement (1985-1990) and published with permission of the Chief Geologist, British Columbia Geological Survey.

We thank Dr. J. A. Mandarino of the Royal Ontario Museum for supplying the platinum-bearing nuggets and Mr. J. M. Beaulne (CANMET) for preparing polished sections. Ms. J. L. Hammack conducted some of the preliminary scanning electron microscope work on the PGM under the guidance of Mr. J. Knight at the University of British Columbia. GTN thanks Dr. P. L. Roeder and Mr. D. Kempson for providing access to, and maintenance of, the microprobe laboratory at Queen's University. We sincerely appreciate the thought-provoking reviews of the manuscript made on short notice by Drs. P. L. Roeder and M. L. Zientek, and the editorial comments and efficiency of Dr. R. F. Martin.

REFERENCES

- ALBEE, A.L. & RAY, L. (1970): Correction factors for the electronprobe microanalysis of silicates, oxides, carbonates and sulfates. *Anal. Chem.* **42**, 1408-1414.
- AMOSSÉ, J., ALLIBERT, M., FISCHER, W. & PIBOULE, M. (1990): Experimental study of the solubility of platinum and iridium in basic silicate melts - implications for the differentiation of platinum-group elements during magmatic processes. *Chem. Geol.* **81**, 45-53.
- BENCE, A.E. & ALBEE, A.L. (1968): Empirical correction factors for the electron microanalysis of silicates and oxides. *J. Geol.* **76**, 382-403.
- BLISS, N.W. & MACLEAN, W.H. (1975): The paragenesis of zoned chromite from central Manitoba. *Geochim. Cosmochim. Acta* **39**, 973-990.
- CABRI, L.J. (1981): Nature and distribution of platinum-group element deposits. *Episodes* **1981-2**, 31-35.
- _____, CRIDDLE, A.J., LAFLAMME, J.H.G., BEARNE, G.S. & HARRIS, D.C. (1981): Mineralogical study of complex Pt-Fe nuggets from Ethiopia. *Bull. Minéral.* **104**, 508-525.
- _____ & FEATHER, C.E. (1975): Platinum-iron alloys: a nomenclature based on a study of natural and synthetic alloys. *Can. Mineral.* **13**, 117-126.
- _____ & HEY, M.H. (1974): Platiniridium - confirmation as a valid mineral species. *Can. Mineral.* **12**, 299-303.
- _____ & LAFLAMME, J.H.G. (1988): Mineralogical study of the platinum-group element distribution and associated minerals from three stratigraphic layers, Bird River sill, Manitoba. *Can. Centre Min. Energy Technol., Rep.* **CM88-1E**.
- _____, OWENS, D.R. & LAFLAMME, J.H.G. (1973): Tulameenite, a new platinum-iron-copper mineral from placers in the Tulameen River area, British Columbia. *Can. Mineral.* **12**, 21-25.
- _____, ROSENZWEIG, A. & PINCH, W.W. (1977): Platinum-group minerals from Onverwacht. 1. Pt-Fe-Cu-Ni alloys. *Can. Mineral.* **15**, 380-384.
- CAMSELL, C. (1913): Geology and mineral deposits of the Tulameen District, British Columbia. *Geol. Surv. Can., Mem.* **26**.
- CLARK, T. (1975): *Geology of an Ultramafic Complex on the Turnagain River, Northwestern British Columbia*. Ph.D. thesis, Queen's Univ., Kingston, Ontario.
- _____ (1978): Oxide minerals in the Turnagain ultramafic complex, northwestern British Columbia. *Can. J. Earth Sci.* **15**, 1893-1903.
- _____ (1980): Petrology of the Turnagain ultramafic complex, northwestern British Columbia. *Can. J. Earth Sci.* **17**, 744-757.
- CORRIVAUX, L. & LAFLAMME, J.H.G. (1990): Minéralogie des éléments du groupe du platine dans les chromitites de l'ophiolite de Thetford Mines. *Can. Mineral.* **28**, 579-595.
- COX, D.P. & SINGER, D.A., eds. (1986): Mineral deposit models. *U.S. Geol. Surv., Bull.* **1693**.
- DUPARC, L. & TIKONOWITCH, M.-N. (1920): *Le Platine et les Gîtes Platinifères de l'Oural et du Monde*. Sonor, Genève.

- EALES, H.V. (1987): Upper Critical Zone chromitite layers at R.P.M. Union Section Mine, western Bushveld complex. *In* Evolution of Chromium Ore Fields (C. W. Stowe, ed.). Van Nostrand Reinhold, New York, N.Y. (144-168).
- EVANS, B.W. & FROST, B.R. (1975): Chrome-spinel in progressive metamorphism - a preliminary analysis. *Geochim. Cosmochim. Acta* **39**, 959-972.
- FINDLAY, D.C. (1963): *Petrology of the Tulameen Ultramafic Complex, Yale District, British Columbia*. Ph.D. thesis, Queen's Univ., Kingston, Ontario.
- _____ (1969): Origin of the Tulameen ultramafic-gabbro complex, southern British Columbia. *Can. J. Earth Sci.* **6**, 399-425.
- GENKIN, A.D. & EVSTIGNEVA, T.L. (1986): Associations of platinum-group minerals of the Noril'sk copper-nickel sulfide ores. *Econ. Geol.* **81**, 1203-1212.
- HARRIS, D.C. & CABRI, L.J. (1973): The nomenclature of the natural alloys of osmium, iridium and ruthenium based on new compositional data of alloys from world-wide occurrences. *Can. Mineral.* **12**, 104-112.
- HEALD, E.F. (1967): Thermodynamics of iron-platinum alloys. *Trans. Metall. Soc. (AIME)* **239**, 1337-1340.
- HILL, R. & ROEDER, P. (1974): The crystallization of spinel from basalt liquid as a function of oxygen fugacity. *J. Geol.* **82**, 709-729.
- IRVINE, T.N. (1965): Chromian spinel as a petrogenetic indicator. 1. Theory. *Can. J. Earth Sci.* **2**, 648-672.
- _____ (1967): Chromian spinel as a petrogenetic indicator. 2. Petrologic applications. *Can. J. Earth Sci.* **4**, 71-103.
- _____ (1974): Petrology of the Duke Island ultramafic complex, southeastern Alaska. *Geol. Soc. Am. Mem.* **138**.
- JOHAN, Z., OHNENSTETTER, M., SLANSKY, E., BARRON, L.M. & SUPPEL, D. (1989): Platinum mineralization in the Alaskan-type intrusive complexes near Fifield, New South Wales, Australia. 1. Platinum-group minerals in clinopyroxenites of the Kelvin Grove prospect, Owendale intrusion. *Mineral. Petrol.* **40**, 289-309.
- LAFLAMME, J.H.G. (1990): The preparation of materials for microscopic study. *In* Advanced Microscopic Studies of Ore Minerals (J.L. Jambor & D.J. Vaughan, eds.). *Mineral. Assoc. Can., Short Course Handbook* **17**, 37-68.
- LEAKE, B.E. (1978): Nomenclature of amphiboles. *Can. Mineral.* **16**, 501-520.
- LEE, C.A. & PARRY, S.J. (1988): Platinum-group element geochemistry of the Lower and Middle Group chromitites of the eastern Bushveld Complex. *Econ. Geol.* **83**, 1127-1139.
- LEGENBRE, O. & AUGÉ, T. (1986): Mineralogy of platinum-group mineral inclusions in chromitites from different ophiolitic complexes. *In* Metallogeny of Basic and Ultrabasic Rocks (M.J. Gallagher, R.A. Ixer, C.R. Neary & H.M. Prichard, eds.). *Inst. Min. Metall.*, London (361-372).
- MAKOVICKY, M., MAKOVICKY, E. & ROSE-HANSEN, J. (1986): Experimental studies on the solubility and distribution of platinum group elements in base-metal sulphides in platinum deposits. *In* Metallogeny of Basic and Ultrabasic Rocks (M.J. Gallagher, R.A. Ixer, C.R. Neary & H.M. Prichard, eds.). *Inst. Min. Metall.*, London (415-425).
- MORIMOTO, N. (1989): Nomenclature of pyroxenes. *Can. Mineral.* **27**, 143-156.
- MORTIMER, N. (1986): Late Triassic, arc-related, potassium igneous rocks of the North American Cordillera. *Geology* **14**, 1035-1038.
- NALDRETT, A.J. (1989): *Magmatic Sulfide Deposits*. Oxford University Press, New York, N.Y.
- _____, CAMERON, G., VON GRUENEWALDT, G. & SHARPE, M.R. (1987): The formation of stratiform PGE deposits in layered intrusions. *In* Layered Intrusions (I. Parsons, ed.). D. Reidel, Dordrecht, Holland. (313-397).
- _____ & LEHMANN, J. (1987): Spinel non-stoichiometry as the explanation for Ni, Cu- and PGE-enriched sulphides in chromitites. *In* Geoplatinum '87 Symp. Vol. (H.M. Prichard, R.J. Potts, J.F.W. Bowles & S.J. Cribb, eds.). Elsevier, London (93-110).
- _____ & VON GRUENEWALDT, G. (1989): The association of PGE with chromitite in layered intrusions and ophiolite complexes. *Econ. Geol.* **84**, 180-187.
- NIXON, G.T. (1988): Geology of the Tulameen ultramafic complex. *B. C. Ministry of Energy, Mines and Petroleum Resources, Open-File Rep.* **1988-25**.
- _____ (1990): Geology and precious metal potential of mafic-ultramafic rocks in British Columbia: current progress. *In* Geological Fieldwork 1989. *B. C. Ministry of Energy, Mines and Petroleum Resources, Pap.* **1990-1**, 353-358.
- _____ & HAMMACK, J.L. (1990): Metallogeny of mafic-ultramafic rocks. *In* Ore Deposits, Tectonics and Metallogeny in the Canadian Cordillera. *Mineral. Dep. Div. of Geol. Assoc. Can., Short Course Notes, Sect.* **5-3**.

- ____ & RUBLEE, V.J. (1988): Alaskan-type ultramafic rocks in British Columbia: new concepts of the structure of the Tulameen Complex. *B.C. Ministry of Energy, Mines and Petroleum Resources, Geol. Fieldwork 1987, Pap.* **1988-1**, 281-294.
- O'NEILL, J.J. & GUNNING, H.C. (1934): Platinum and allied metal deposits of Canada. *Geol. Surv. Can., Econ. Geol. Ser.* **13**.
- PAN, YUANMING & FLEET, M.E. (1989): Cr-rich calcisilicates from the Hemlo area, Ontario. *Can. Mineral.* **27**, 565-577.
- PRICHARD, H.M., NEARY, C.R. & POTTS, P.J. (1986): Platinum group minerals in the Shetland ophiolite. In *Metallogeny of Basic and Ultrabasic Rocks* (M.J. Gallagher, R.A. Ixer, C.R. Neary & H.M. Prichard, eds.). Inst. Min. Metall., London (395-414).
- RAICEVIC, D. & CABRI, L.J. (1976): Mineralogy and concentration of Au- and Pt-bearing placers from the Tulameen River area in British Columbia. *Can. Inst. Min. Metall. Bull.* **69**(770), 111-119.
- RICE, H.M.A. (1947): Geology and mineral deposits of the Princeton map-area, British Columbia. *Geol. Surv. Can., Mem.* **243**.
- ROEDER, P.L. & CAMPBELL, I.H. (1985): The effect of postcumulus reactions on composition of chromespinels from the Jimberlana intrusion. *J. Petrol.* **26**, 763-786.
- RUBLEE, V.J. & PARRISH, R.R. (1990): Chemistry, chronology and tectonic significance of the Tulameen complex, southwestern British Columbia. *Geol. Assoc. Can. - Mineral. Assoc. Can., Program Abstr.* **15**, A114.
- ST. LOUIS, R.M., NESBITT, B.E. & MORTON, R.D. (1986): Geochemistry of platinum-group elements in the Tulameen ultramafic complex, southern British Columbia. *Econ. Geol.* **81**, 961-973.
- STOCKMAN, H.W. & HLAVA, P.F. (1984): Platinum-group minerals in Alpine chromitites from southwestern Oregon. *Econ. Geol.* **79**, 491-508.
- TALKINGTON, R.W. & WATKINSON, D.H. (1986): Whole-rock platinum-group element trends in chromite-rich rocks in ophiolitic and stratiform igneous complexes. In *Metallogeny of Basic and Ultrabasic Rocks* (M.J. Gallagher, R.A. Ixer, C.R. Neary & H.M. Prichard, eds.). Inst. Min. Metall., London (427-440).

Received June 24, 1990, revised manuscript accepted August 10, 1990.